International Institute for Applied Systems Analysis
IIASA www.iiasa.ac.at

An Approach to Uncertainty of a Long Range Air Pollutant Transport Model

Alcamo, J. and Bartnicki, J.

IIASA Working Paper

WP-85-088

December 1985

Working Paper

AN APPROACH TO UNCERTAINTY OF A LONG RANGE AIR POLLUTANT TRANSPORT MODEL

Joseph Alcamo
Jerzy Bartnicki

December 1985
WP-85-88

International Institute for Applied Systems Analysis
A-2361 Laxenburg, Austria

AN APPROACH TO UNCERTAINTY OF A LONG RANGE AIR POLLUTANT TRANSPORT MODEL

Joseph Alcamo
Jerzy Bartnicki

December 1985
WP-85-88

INTERNATIONAL INSTITUTE FOR APPLIED SYSTEMS ANALYSIS
2361 Laxenburg, Austria

PREFACE

One of the goals of IIASA's Acid Rain project is to create a model that could be used in negotiations about control strategies for acid deposition between European countries. To that end it is necessary that the model builders present the model users a clear picture of the credibility of the model. One way to maximize credibility would be to create a very complex model with as many as possible (mostly non-linear) relationships. Our strategy has been another one: construct a simple model and evaluate its uncertainties. Thus uncertainty analysis forms an important part of the Acid Rain project's research agenda. This paper describes a general framework for our uncertainty analysis. Moreover the authors have applied the framework to the atmospheric submodel of our RAINS (Regional Acidification Information and Simulation) model. I am convinced that this paper not only is a substantial contribution to evaluation of the credibility of RAINS, but that it is also of importance for the further development of the long range transport model which is incorporated in RAINS and has been built by the Norwegian Institute of Meteorology under the Co-operative Programme for Monitoring and Evaluation of the Long-Range Transmission of Air Pollutants in Europe (EMEP).

This paper is the product of a collaboration with the Institute for Meteorology and Water Management in Warsaw (Poland) under a study contract "Analysis of Uncertainty in Modeling Atmospheric Processes".

Leen Hordijk
Project Leader

ACKNOWLEDGEMENTS

Wolfgang Schöpp developed the computer program for the Monte Carlo simulation described herein. Maximilian Posch conducted the analysis of EMEP source-receptor matrices. The authors also wish to acknowledge the contributions of Roel van Aalst, Ruwin Berkowicz, Gode Gravenhorst, Sylvain Joffre, Annikki Mäkelä, Göran Nordlund, Sergei Pitovranov and Joop den Tonkelaar to the ideas presented in this paper. The authors are grateful for the great amount of assistance provided by Anton Eliassen and Jorgen Saltbones through the Meteorological Synthesizing Center-West. Leen Hordijk and Maximilian Posch gratefully reviewed the entire manuscript of this paper. Work described in this paper was supported, in part, by a collaborative agreement between IIASA and the Institute of Meteorology and Water Management in Warsaw, with Dr. Jerzy Pruchnicki as Polish coordinator of the agreement. Vicky Hsiung typed the manuscript of this paper.

ABSTRACT

This paper presents a preliminary framework for analyzing uncertainty of a long range air pollutant transport model. This framework was used to assess EMEP model uncertainty. The uncertainty problem is defined in a decision-making context and a distinction is made between uncertainty analysis, sensitivity analysis, and model calibration/verification. A taxonomy is introduced to organize uncertainty sources. The taxonomy includes: ***model structure***, ***parameters***, ***forcing functions***, ***initial state*** and ***model operation***. These categories are further subdivided into ***diagnostic*** and ***forecasting*** components. To limit the number of uncertainties for quantitative evaluation, some uncertainties are "screened". Methods are introduced to evaluate uncertainties. These include (1) Monte Carlo simulation of composite parameter, forcing function and initial state uncertainties, and (2) statistical analysis of EMEP source-receptor matrices. Preliminary results of applying this methodology to the EMEP model are presented.

TABLE OF CONTENTS

AN APPROACH TO UNCERTAINTY OF A LONG RANGE AIR POLLUTANT TRANSPORT MODEL

Joseph Alcamo and Jerzy Bartnicki

1. INTRODUCTION

Along with the recognition of regional and interregional air quality problems, came the need for new tools to analyze these problems. Among these new tools are atmospheric long range transport models which help to establish the relationship between pollutant emissions and their deposition hundreds or thousands of kilometers away. The importance given to these models by the scientific community is clear from recent national and international publications (see, e.g., OECD (1979), U.S. National Research Council (1983), MOI (1982)).

A key issue in using these and other air pollution models for decision making (any mathematical model, for that matter) is the credibility of the model's results. An essential aspect of this credibility is how well the model user understands the model's uncertainty. This paper presents a framework

to comprehensively treat the uncertainty of long range transport of air pollutants models (sometimes referred to as LRTAP models) and applies this framework to the analysis of uncertainty of the so-called EMEP model* (Eliassen and Saltbones, 1983). From a larger perspective, we believe that the framework presented herein can be generally applied to other types of environmental models. Throughout the paper we (1) discuss key issues concerned with uncertainty analysis, (2) present numerical examples of different aspects of this analysis based on preliminary results from the IIASA Acid Rain Project, (3) denote future work that will be conducted within the frame of the IIASA Project. Since this research is only in its early stages, we intend this to be a ***discussion paper***.

In this paper we are specifically interested in ***determining the uncertainty of using model results in a decision-making context***. Our goals for the uncertainty analysis include:

1. To quantify, where possible, the combined uncertainties of many different uncertainty sources, i.e. determine the uncertainty range of model calculations.
2. To determine under what conditions the model performs best.
3. To make more explicit the assumptions behind model parameters, forcing functions, etc.
4. To identify the sources and relative importance of uncertainties as a guide to model use and setting research priorities.

*The EMEP model is described in Section 3.2 of this paper.

The analysis reported in this paper builds on previous work on model uncertainty in the fields of decision analysis (cf. Howard and Matheson, 1983) and econometrics (cf. Griliches and Intrilligator, 1983), as well as investigations in water quality modeling (cf. Fedra, 1983 and Beck and Van Straten, 1983) and ecological modeling (cf. Gardner et al, 1982). Compared to these fields, much less quantitative analysis has been conducted on atmospheric model uncertainty. A notable exception is the work done at Carnegie-Mellon University (Morgan et al, 1984). Also, a report from an American Meteorological Society Workshop outlines some key issues in the quantitative assessment of atmospheric models (Fox, 1984). Unfortunately a review of the aforementioned work is outside of this paper's scope.

1.1. Uncertainty and Model Credibility

Model credibility is based on several ill-defined criteria. One criterion is the *scientific basis* of the model equations, i.e. the soundness of the physical/chemical/biological concepts behind the model. Another is *verification* and *validation*, generally meaning the comparison of model results with observations and the examination of model behavior to see if it is realistic. Still another way to enhance the credibility of model results is to perform sensitivity analysis. Collectively, these approaches make model users *more* confident in using a model yet they do not specifically address the question of the *uncertainty* of model results. In this sense *model uncertainty* is the departure of model calculations from current or future "true values". Mathematically, our meaning of uncertainty can be expressed as the following.

Let us assume that an environmental model can be expressed* as:

$$\mathbf{Y} = \hat{G}(\mathbf{X}) \tag{1.1}$$

where

$\mathbf{Y} = (y_1,\ldots,y_n)$ is an output vector (model results)

$\mathbf{X} = (x_1,\ldots,x_m)$ in an input vector (input model variables)

$\hat{G}$ is an operator (usually a differential).

Since the input vector usually contains variables which are dependent on space and time, the output vector is also a function of space and time. In addition, output variables depend on some constants in time and space, i.e. parameters.

If we assume now, that "true values" of the output variables are represented by vector $\mathbf{Y}'$, the model uncertainty can be defined as:

$$\varepsilon = \mathbf{Y} - \mathbf{Y}' \tag{1.2}$$

where:

$$\varepsilon = (\varepsilon_1,\ldots,\varepsilon_i,\ldots,\varepsilon_n)$$

$$\mathbf{Y}' = (y_1',\ldots,y_i',\ldots,y_n')$$

$$\varepsilon_i = y_i - y_i'$$

It should be mentioned here, that it is extremely difficult to compute the complete uncertainty vector because, among other reasons, "true values" are illusive. There are ways however to circumvent this problem. Repeated comparisons of observed versus model computations (model

---

*Even though the model definition used in this paper is not the the most general possible, it is still general enough for most of the environmental models.

calibration/verification) yields insight to ε, though in sections 1.2 and 6.1 we discuss drawbacks to this approach. Another strategy, which is discussed in Section 6.3, is to assess the uncertainty of the **X** vector in (1.1), and compute a new **Y**. This provides an indirect estimate of ε. Other strategies are reviewed in the text.

The equation (1.2) used here to define uncertainty is related as well to *model calibration/verification*. However, the important difference is, that in the case of model calibration/verification, the components of the vector **Y** have to be *measurable*, while in case of uncertainty, this is not necessary. In this sense our definition of uncertainty is more general.

1.2. Sensitivity Analysis and Calibration/Verification

Though "sensitivity analysis" and "model calibration/verification" are relevant to a model's uncertainty, both approaches have limitations.

Sensitivity analysis in the conventional sense* is difficult to perform for two or more variables and tends to emphasize extreme events. It is different from model uncertainty because sensitivity analysis is interested in the incremental changes of model results caused by an incremental change in input variables. In fact, the objective of most *sensitivity* analyses is, of course, to determine the relative importance of one independent variable compared to another; not how much model calculations depart from reality. In this sense sensitivity analysis is an essential part of model development. Mathematically we can express sensitivity analysis as a procedure for com-

*Rather than add yet another definition of sensitivity analysis we quote a published definition: "Sensitivity analysis involves ... making a series of runs with a model and noting the magnitude of the changes in results as assumptions, parameters and initial conditions are changed in an orderly fashion." (McLeod, 1982, p. 96).

puting matrix S:

$$\mathbf{S} = \frac{\delta Y}{\delta \mathbf{X}} \tag{1.3}$$

The elements of the sensitivity matrix $\mathbf{S} = [s_{ij}]$ are given by the relation:

$$s_{ij} = \frac{\delta y_i}{\delta x_i}; \; i = 1,\ldots,m; \; j = 1,\ldots,n \tag{1.4}$$

Model calibration/verification, i.e. comparison of model output with observations has the following limitations in assessing model uncertainty:

(i) *Observations are often unreliable.* Eliassen and Saltbones (1983) present one example of analytical errors in sulfate data used to check EMEP model calculations.

(ii) *Model output is not necessarily "observable" in nature, especially if the model describes an aggregated system.* For models with large temporal/spatial resolution such as the EMEP model, it is difficult to rely on comparisons of model output with observations. Strictly speaking, since the EMEP model computes SO_2 gas and $SO_4^=$ in rain over 150 km long orthogonal coordinates and a 1 km vertical mixing layer, model output should be checked with observations averaged over the same spatial scale. This class of error is termed *aggregation* error and has been dealt with in some detail in the ecological modeling literature (Gardner, et al, 1982). A related problem occurs when an important model output is virtually unobservable as in the case of total sulfur deposition.

(iii) *Certain cause-effect relations may not be readily observable.* An example of this is the relationship between sulfur emissions from a particular country and its deposition at a particular location in

Europe. Though wind sector analysis may help to quantify this relation for short periods of time, it is difficult to do so over a longer time scale, say one year. Nevertheless this time scale and relationship is computed by the EMEP model and is of particular importance in decision making.

(iv) *Agreement of model output with data does not settle the question of model uncertainty when the model is used for forecasting purposes.* For example, model agreement with observations does not address the impact of interannual meteorological variability on the uncertainty of model forecasts.

(v) *Sometimes model parameters can be "artificially tuned" such that model output closely agrees with data.* Under these circumstances it may appear that the model has little or no uncertainty, although the uncertainty has simply been transferred to the uncertainty in choosing the correct parameters for forecasting purposes.

(vi) *It is often difficult to assemble data for a comprehensive range of environmental conditions.* Even though we test the model against data from several time periods, we still may have low confidence that we have covered a representative range of environmental conditions.

Despite the preceding caveats, model calibration/verification remains the only sure "benchmark" of a model's relationship to reality. As such, *model calibration/verification* together with *sensitivity analysis* is *necessary and useful though insufficient* in evaluating environmental

model uncertainty. In the following sections we propose a comprehensive framework to assess model uncertainty which incorporates elements of both model calibration/verification and sensitivity analysis.

2. PROPOSED FRAMEWORK

A comprehensive approach to analyze long range transport model uncertainty should include the following:

(i) *Problem Formulation* - Despite the trivial nature of this step it is surprising how often investigators discuss uncertainty of a model without specifying the time and space scales of interest. In Section 7.2 of this paper we present an example of the dependence of model uncertainty on the temporal-spatial dimensions of the problem. Before proceeding with an uncertainty analysis it is therefore vital to carefully formulate the problem of interest.

(ii) *Inventory of Uncertainty* - In this step we assemble and classify the sources of uncertainty for further analysis. Our goal is to list as comprehensively as possible every major source of uncertainty. To do this we propose a taxonomy of model uncertainty in Section 4.1 of this paper.

(iii) *Screening and Ranking of Uncertainty* - Virtually every model used to describe a real system will have a very large number of uncertainties. To limit the sources of uncertainty for quantitative evaluation we try in this step to identify the most important sources. This is accomplished through conventional sensitivity analysis or qualitative judgement and need not have time-space scales identical to those in step number one.

(iv) *Evaluation of Uncertainty* - The sources of uncertainty which remain after step (iii) can be evaluated by a number of different quantitative techniques. Sections 6 and 7 describes some

approaches being taken in the IIASA Acid Rain Project's analysis of EMEP model uncertainty.

(v) *Application to Decision Making* - Once an estimate of uncertainty is derived in step (iv), we still must interpret this estimate in a way useful to decision making. For example, we could express the uncertainty of EMEP calculations of sulfur deposition as spatial variations of deposition isolines, or as deposition ranges around individual isolines. Alternatively we could apply an "average" uncertainty estimate to each EMEP grid element. These and other alternatives are addressed in Section 8 of this paper.

3. PROBLEM FORMULATION

3.1. Time and Space Scales

The degree to which uncertainty can vary depending on spatial-temporal scales is illustrated in Figure 7.1 which summarizes an analysis of uncertainty in computed sulfur deposition due to interannual variation of precipitation and wind patterns. Since we have specified above that we are interested in "determining the uncertainty of using model results in a decision-making context", we must now clarify the time and space scales relevant to decision-making. First, we assume that we are interested in a specific *source-receptor* relationship for sulfur emissions, sulfur deposition and air concentration. Next we assume that the country-scale is the appropriate spatial-scale for sulfur emission sources because (1) most countries in Europe report their sulfur emissions as country totals, although a few report additional spatial information, (2) most proposed international control policies (for example, the "Thirty Percent Club") refer to country-scale sulfur emissions. The EMEP grid element is an appropriate spatial scale for receptor sulfur deposition since a coarser resolution would be unsuitable for analyzing known spatial variations of environmental impact (such as forest damage) which occurs within countries. In addition, since a model for analyzing international control policies in Europe should cover all of Europe, a spatial scale much smaller than 150 km may increase the number of computational steps to an unacceptable level. Moreover, the spatial resolution of meteorological data in Europe is also approximately 10^4 km^2.

The time scale of the source-receptor relationship should take into account that confidence of any air pollution model increases with the averaging period of results*. In addition, the time step should be compatible with the long time period and broad spatial coverage needed for policy analysis. With these considerations in mind, an annual time step is taken to be an appropriate scale. This time step is also appropriate for assessing forest damage since most field studies record annual pollutant deposition or air concentration.

We may summarize the discussion to this point by specifying the source-receptor time resolution as *one* year, *country-scale* as the spatial resolution for sulfur emissions, and *EMEP grid element* as the spatial resolution for sulfur deposition and air concentration. The relationship of interest, therefore, between deposition and sulfur emissions can be expressed as:

$$d_{ij} = s_i \, a_{ij} \tag{3.1a}$$

where

d_{ij} = total sulfur deposition at grid element j due to country i ($g\ S\ m^{-2}\ yr^{-1}$)

s_i = total sulfur emissions from country i ($t\ S\ yr^{-1}$)

a_{ij} = element of source-receptor matrix

We define our uncertainty $\varepsilon_{d_{ij}}$ of deposition as

$$\varepsilon_{d_{ij}} = d_{ij} - d'_{ij} \tag{3.1b}$$

where d'_{ij} is the "true" deposition.

*As an example, one EMEP review states that the model "continued to demonstrate its effectiveness in modelling air concentrations and depositions when averaged over seasons or years" (WMO, 1983).

We are also interested in the uncertainty of the total deposition at grid element j (where b_j is background deposition):

$$d_j = \sum_{i=1}^{27} a_{ij}\, s_i + b_j \qquad (3.2a)$$

for $j = 1, \cdots m$

and

$$\varepsilon_{d_j} = d_j - d_j' \qquad (3.2b)$$

The same form of equations (3.1a) through (3.2b) can be applied to the other EMEP state variables (e.g. SO_2 air concentration). These other state variables will be introduced in the next section.

It follows from the above that we are interested in the uncertainty of computed annual sulfur deposition at various locations in Europe, where these locations are defined by EMEP grid elements. This can be expressed either as an uncertainty range around a linear source-receptor relationship (Figure 3.1) or a frequency distribution of computed sulfur deposition (Figure 3.2). In summary, equations (3.1) and (3.2) define our uncertainty problem. Figures 3.1 and 3.2 illustrate this problem graphically.

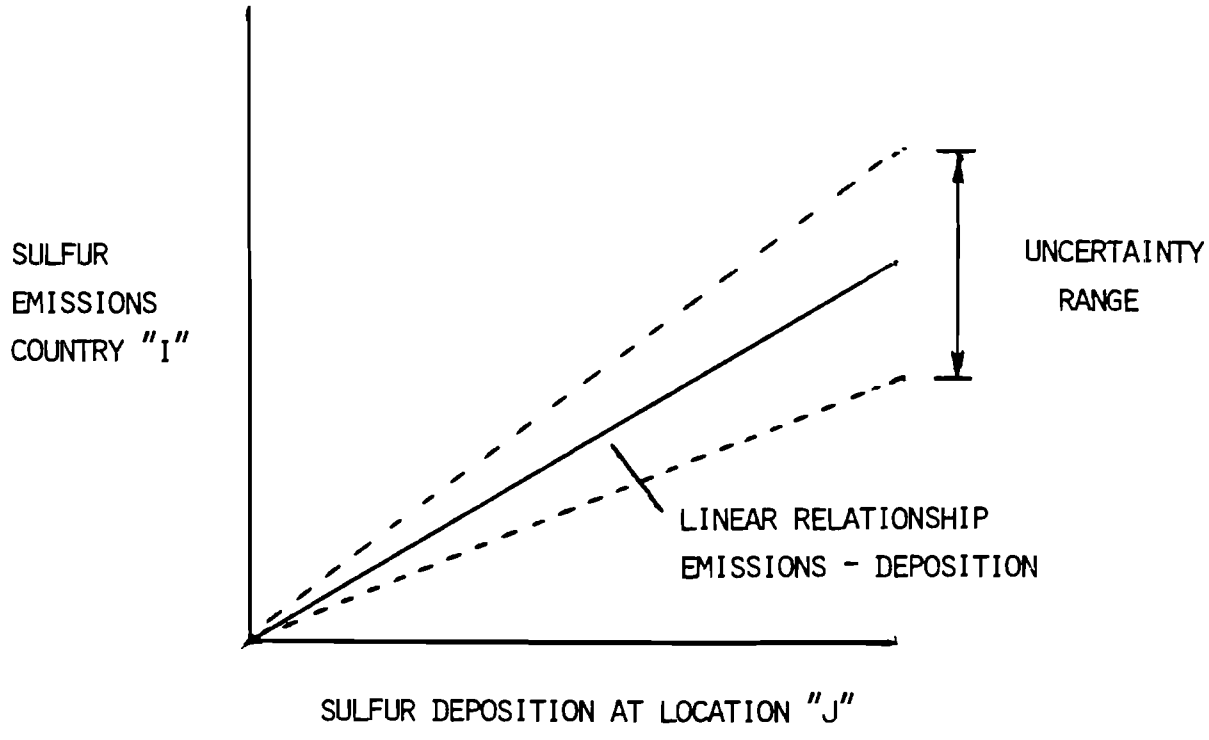

Figure 3.1. Source receptor uncertainty.

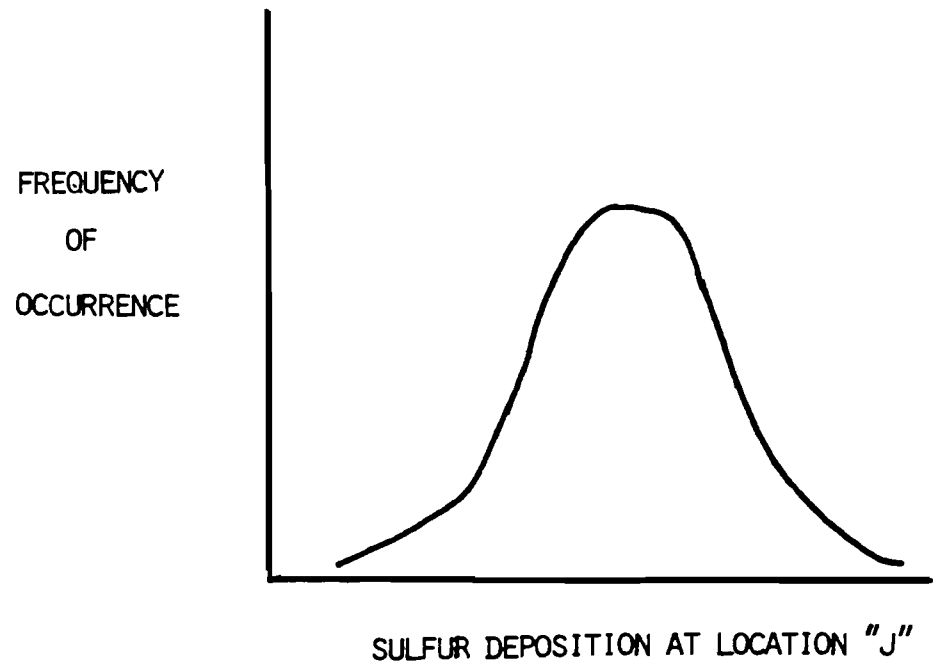

Figure 3.2. Frequency distribution of computed deposition.

3.2. EMEP Model Description

A general form of the EMEP model is:

$$\frac{\partial c}{\partial t} = -\left(u\,\frac{\partial c}{\partial x} + v\frac{\partial c}{\partial y}\right) + R_i + Q_i \qquad (3.3)$$

where

$\frac{\partial c}{\partial t}$ = change in concentration with time.

u, v = orthogonal wind velocities.

$\frac{\partial c}{\partial x}, \frac{\partial c}{\partial y}$ = orthogonal concentration gradients.

R_i = change in concentration due to chemical reactions and sink processes.

Q_i = pollutant emissions.

The EMEP model uses a Lagrangian approach to solve equation (3.3). Concentrations of SO_2 and $SO_4^=$ are computed along a moving frame of reference. The computation procedure consists of two steps. Trajectories are first calculated, and then mass-conservation equations are solved on these trajectories to compute the concentrations at the receptor point. An additional procedure is used for computing dry and wet deposition of sulfur.

The theoretical formulation of the EMEP model is described by Eliassen and Saltbones (1975) and Eliassen (1978). This model is similar to the one used in the OECD program (OECD, 1979). The main difference is that the EMEP model is based on trajectories followed for 96 hours instead of 48 hours, and grid size of 150 km instead of 127 km.

3.2.1. Determining Air Trajectories

A trajectory can be considered as the path of an air parcel followed by the wind. In the EMEP model two-dimensional trajectories are calculated which neglect vertical motion of the air. The wind field from the 850 hPa level is assumed to be the transport wind within the mixing layer. Petterssen's method (Petterssen, 1956) was chosen for numerical computations of the trajectories. If $\bar{x}$ is the position of the trajectory at time t, the next position $\bar{x} + \Delta\bar{x}$ is calculated using the wind field $\bar{v}(\bar{x},t)$ as follows. Let $\Delta\bar{x}_0$ be the first estimate for the position increment $\Delta\bar{x}$:

$$\Delta\bar{x}_0 = \bar{v}(\bar{x},t)\,\Delta t \tag{3.4}$$

The i-th estimate $\Delta\bar{x}_i$ for Δx is:

$$\Delta\bar{x}_i = \frac{1}{2}(\Delta\bar{x}_0 + \bar{v}(\bar{x} + \Delta\bar{x}_{i-1}, t + \Delta t)\,\Delta t) \tag{3.5}$$

New estimates for $\Delta\bar{x}$ are computed until:

$$\left|\Delta\bar{x}_i - \Delta\bar{x}_{i-1}\right| < \varepsilon \left|\Delta\bar{x}_{i-1}\right| \tag{3.6}$$

where ε is a small positive number equal 0.003 in the EMEP model. If the condition (3.6) is satisfied for i-th estimate then:

$$\Delta\bar{x} = \Delta\bar{x}_i \tag{3.7}$$

The time step Δt is 2 hours, which means that each trajectory is represented by a set of 49 discrete points, including the receptor point. This procedure is sufficiently fast and in most cases condition (3.6) is quickly satisfied.

3.2.2. Model Area, Emissions and Meteorological Data

The coverage of the EMEP model is shown on Figure 3.3. It covers all Europe, a large part of the Atlantic Ocean and a small part of Northern Africa. The numerical grid system has 39 points in the x-direction and 37 in the y-direction. As was mentioned earlier, the grid size is 150 km. The grid elements are identified by the coordinates (i,j). The relation between geographical latitude φ, and longitude λ and a point (i,j) is given by the equations:

$$\varphi = 90 - \frac{360}{\pi} Arctan \frac{r}{\frac{R}{d}(1 + \sin\frac{\pi}{3})} \tag{3.8}$$

$$\lambda = -32 + \frac{180}{\pi} Arctan \frac{i - 3}{37 - j} \tag{3.9}$$

where

$1 < i < 39$ and $1 < j < 37$

$r = \sqrt{(i - 3)^2 + (j - 37)^2}$

(the coordinate of the Northern Pole is (3,37))

R = 6370km - radius of the Earth

d = 150 km - grid size

All meteorological and emissions data are given in the grid system denoted by equations (3.8) and (3.9). The meteorological data are: wind field at 850 hPa level - every 6 hours (with linear interpolation in-between), and precipitation for the last 6 hours. In the routine computations emission data were taken from an inventory prepared by Dovland and Saltbones (1979). Seasonal variation of emission is introduced into the model calculations. It has a shape of sinusoidal function with amplitude 30% and maximum in the beginning of January.

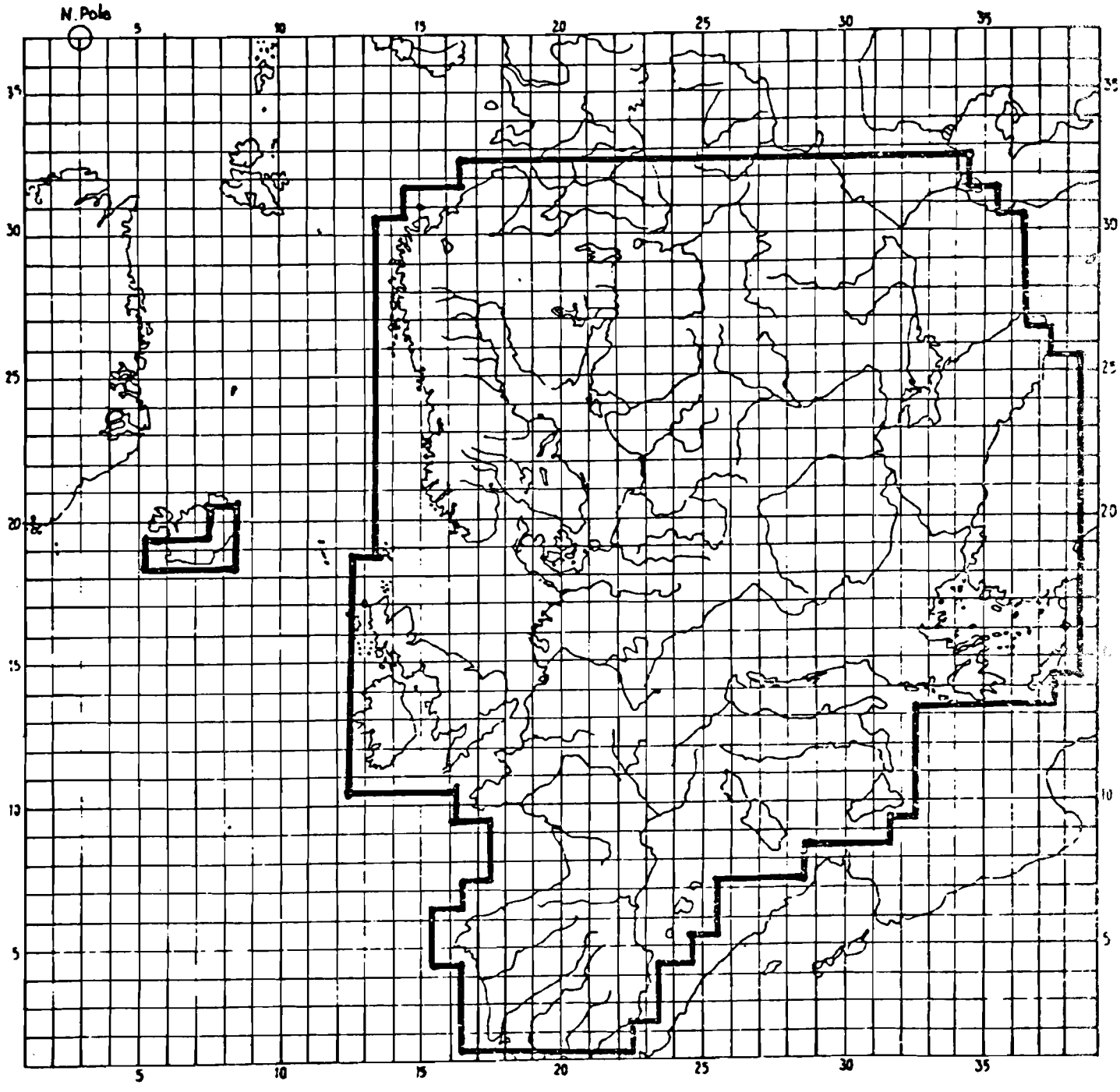

Figure 3.3: Area covered by the EMEP model calculations. Trajectories are followed from arrival points within heavy line.

Concentrations of SO_2 and $SO_4^=$ and dry and wet deposition of sulfur are computed for the entire grid system.

3.2.3. SO_2 and $SO_4^=$ Concentrations

Emissions are computed by linear interpolation in each of 49 points from the four nearest grid points, and occurrence of precipitation is checked. Having this information, equations for SO_2 and $SO_4^=$ can be solved. Denoting SO_2 concentration by c_1 and $SO_4^=$ concentration by c_2 (both measured in sulfur units), we can write these equations in the following form:

$$\frac{Dc_1}{dt} = -\left(\frac{v_d}{h} + k_t + k_w\right)c_1 + (1 - \alpha - \beta)\frac{Q}{h} \tag{3.10}$$

$$\frac{Dc_2}{dt} = -\kappa c_2 + k_t c_1 + \beta\frac{Q}{h} \tag{3.11}$$

The operator $\frac{D}{dt}$ is the total time derivative, Q is sulfur emission per unit area and time. Values for all other symbols and parameters in equations (3.10) and (3.11) are given in Table 3.1.

Table 3.1. Parameter values in the EMEP long-range transport model (from Eliassen and Saltbones, 1983).

Notation	Explanation	Parameter value	Parameter unit
v_d	Deposition velocity for SO_2	8×10^{-3}	$m\ s^{-1}$
v_{ds}	Deposition velocity for $SO_4^=$	2×10^{-3}	$m\ s^{-1}$
h	Mixing height	1000	m
k_t	Transformation rate of SO_2 to $SO_4^=$	2×10^{-6}	s^{-1}
k_w	Wet deposition rate of SO_2, used only in grid elements and six-hour periods when it rains	3×10^{-5}	s^{-1}
α	Additional dry deposition in the same grid square where emission occurs	0.15	*nondimensional*
β	Part of sulfur emission assumed to be emitted directly as sulfate	0.05	*nondimensional*
κ	Overall decay rate for $SO_4^=$	4×10^{-6}	s^{-1}
a	Proportionality coefficient in equation (3.13)		
	In Finland and Norway	0.27×10^{6}	*nondimensional*
	In other countries	0.69×10^{6}	*nondimensional*
b	Background concentration in equation (3.13)		
	In Finland and Norway	0.27	$mg\ S\ l^{-1}$
	In other countries	0.40	$mg\ S\ l^{-1}$

Equations 3.10 and 3.11 are ordinary linear equations solved for a particular trajectory. In regions where precipitation occurs either constantly or not at all, there is also the analytical solution for these equations presented by Eliassen (1978).

3.2.4. Deposition of Sulfur

Dry deposition of sulfur is computed by applying deposition velocities to SO_2 and $SO_4^=$ concentrations:

$$d_d = (\bar{c}_1 \cdot v_d + c_2 v_{ds})\, T \qquad (3.12)$$

where:

d_d =dry deposition of sulfur during time T

T = period of the transport (T= usually 1 year in the EMEP model).

and other variables are as previously defined.

In the routine model wet deposition is not calculated directly from the mass-conservation equations 3.10 and 3.11, because of the constant k_w rate. It is estimated by an indirect method instead, in which the mean concentration of sulfur in precipitation $\hat{c}_3$ is estimated from the computed mean concentration of sulfate during the rain $\hat{c}_2$ using a linear empirical relationship:

$$\hat{c}_3 = a\,\hat{c}_2 + b \qquad (3.13)$$

where $\hat{c}_2$ and $\hat{c}_3$ are averaged over time T. The precipitation-weighted mean $\hat{c}_2$ is calculated from

$$\hat{c}_2 = \frac{1}{P} \sum_i p_i \cdot c_{2,i}$$

where p_i is the amount of precipitation observed on day i, $c_{2,i}$ is the corresponding calculated daily mean air concentration of $SO_4^=$ and P is the total amount of precipitation during time T in a specific grid element. Days without precipitation do not contribute to $\hat{c}_2$.

The empirical proportionality coefficient a in (3.13) corresponds to a scavenging ratio for anthropogenic sulfate. The constant b accounts for background concentration in the rain. The values of a and b are also given in Table 3.1.

The value of the wet deposition in the model d_w is computed as:

$$d_w = \hat{c}_3 \cdot P \tag{3.14}$$

and total deposition of sulfur d_w is:

$$d_t = d_d + d_w \tag{3.15}$$

Units of d_d, d_w, and d_t are in $g \cdot m^{-2}$. In order to compute the mass deposited in a grid element, the values of the deposition must be multiplied by the area of the grid element.

4. INVENTORY OF UNCERTAINTY

4.1. Taxonomy

After formulating our uncertainty problem in Section 3 of this paper, we now wish to assemble and classify the sources of uncertainty. To assist in this classification we propose the following taxonomy of model uncertainty:

(1) Model Structure

(2) Parameters

(3) Forcing Functions

(4) Initial State

(5) Model Operation.

Uncertainty due to *Model Structure* results from imperfect or inaccurate representation of reality by a model. In this sense model structure is taken as the collection of model variables and parameters together with their relationships.

Parameters are defined as those variables which are constant in either time or space, are usually estimated or confirmed as part of the model calibration, and are meant to approximate a more complicated process.

Forcing function in this taxonomy is a model variable which inherently changes in time and space, serves as input for model calibration, and is assumed to be well known (or at least better defined) compared to parameters.*

*Forcing function corresponds to the concept of *input disturbance* in systems science terminology and *exogenous variable* in econometric terminology.

Initial State uncertainty results from the error in assigning boundary and initial conditions.

Finally, uncertainty due to *Model Operation* refers to errors in the solution techniques of model equations or in processing model input and output, e.g. numerical error arising from approximation of differential equations and interpolation of model input and output. The sum of forcing function and initial state errors can also be termed *input uncertainty*.

Each of the above categories can be further sub-divided into two additional classes: *diagnostic* uncertainty and *forecasting* uncertainty. *Diagnostic* uncertainty pertains to model use in simulating past and current conditions. *Forecasting* uncertainty arises when the model is used to estimate future conditions.** Each source of uncertainty (according to the model taxonomy, presented above) has both a diagnostic and forecasting component.

Before proceeding with the application of the above taxonomy to the EMEP model, we note that this taxonomy is hierarchically organized as illustrated in Figure 4.1. This figure notes that uncertainties due to parameters, forcing functions, initial state and model operation depend on model structure. As an example, let us assume that we are uncertain of the exact value of the dry deposition velocity v_d in the EMEP model, but can estimate its interval as $[v_d]$. We then estimate the uncertainty of computed sulfur deposition by using, for example, a Monte Carlo technique described in Section 6.3. This computed uncertainty will depend on the form and content of the

**Other investigators use different terms to make the same distinction. For example, Beck (1983) uses *Identification* and *Prediction*.

model equations, i.e. the model structure. Thus it is unlikely that the uncertainty of Model 'A' will be exactly the same as the uncertainty of Model 'B' even if both models use duplicate environmental conditions and parameters values, etc., as input. This idea is illustrated in Figure 4.2. In other words, quantitative estimates of uncertainty due to parameters, etc., pertain only to a particular model.

Figure 4.3 also notes that parameter, etc., uncertainty depends on environmental conditions. This is also obvious if we consider that the uncertainty of v_d will have a small influence on computed sulfur deposition if conditions are very wet, i.e. if wet deposition is the predominant sulfur removal mechanism. For drier conditions the reverse will be true. This implies that conclusions about model uncertainty must always include information about the environmental conditions under which these uncertainty estimates were made. This leads to the concept of a "frequency distribution of uncertainty" and "expected value of uncertainty", illustrated in Figure 4.4.

Of course if the departure of model calculations from observations is relatively constant for many different environmental conditions, then we may suspect that ε will also not vary very much for different environmental conditions.

4.2. Application to EMEP Model

The diagnostic and forecasting uncertainties due to ***model structure*** will be the same if the system doesn't change, i.e. if the model contains the dominant variables and interrelationships of the real system for both future and current conditions. However, if for example the air concentrations of co-pollutants such as O_3 or NO_2 increase such that they affect the transfor-

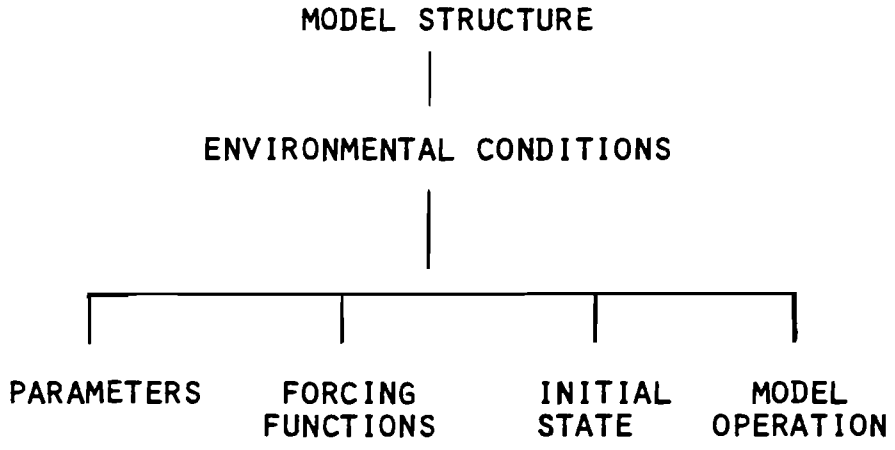

Figure 4.1. **Hierarchy of model uncertainty**

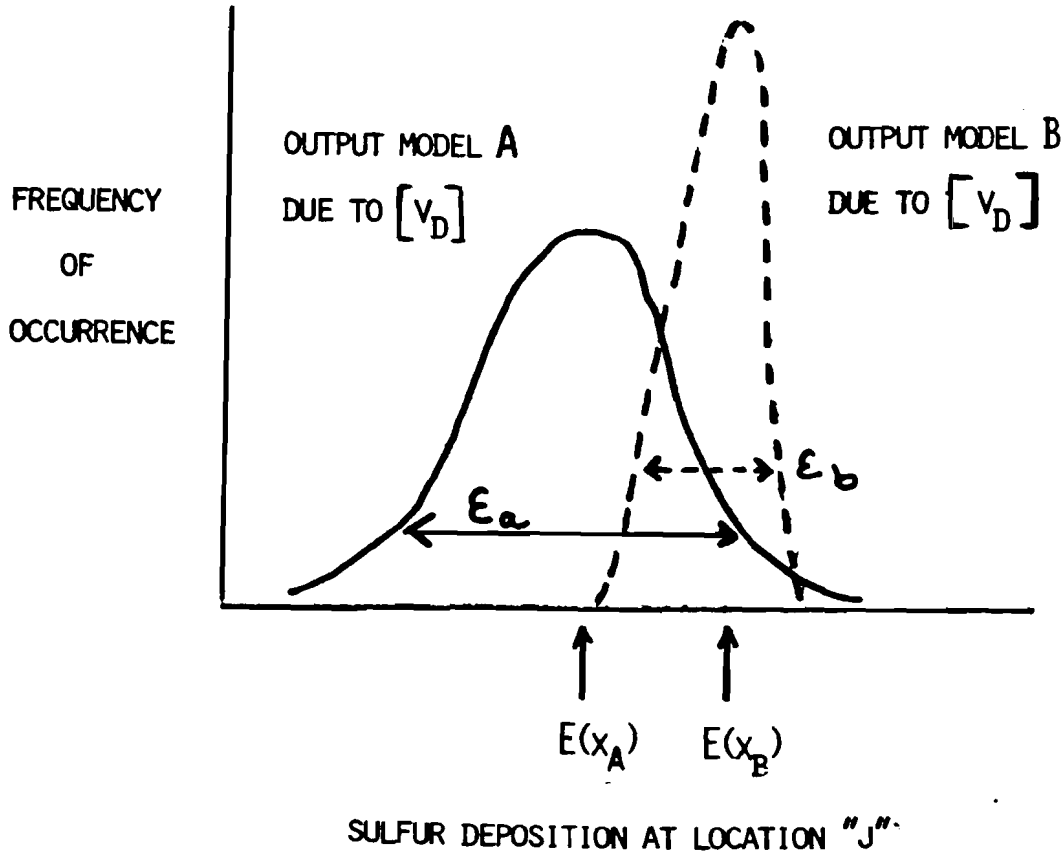

Figure 4.2. Uncertainty (ε) depends on model structure.

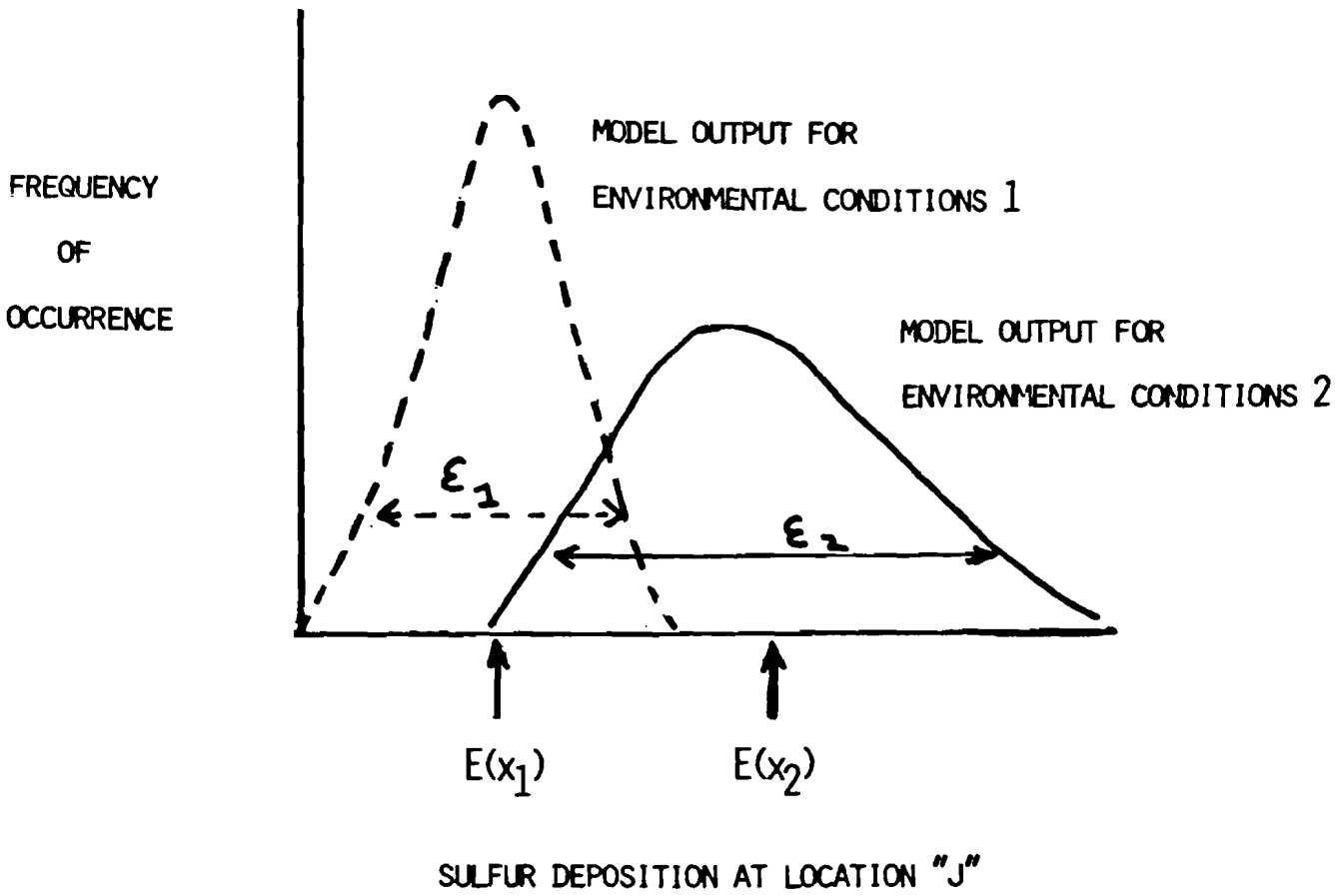

Figure 4.3. Uncertainty (ε) depends on environmental conditions.

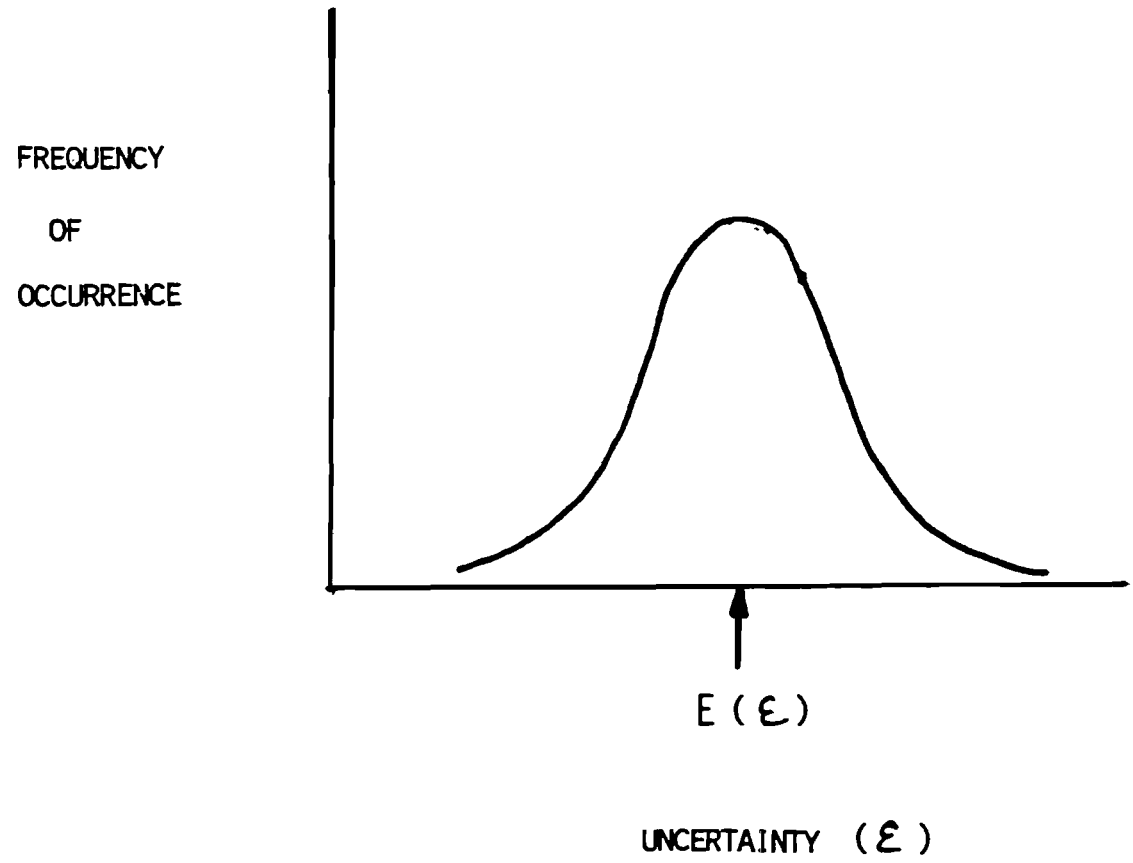

Figure 4.4. **Frequency distribution of uncertainty (ε) for a range of environmental conditions.**

mation of SO_2 or $SO_4^=$, then a new model structure may be required with new variables and parameters. This implies that forecasting and diagnostic uncertainty due to model structure will be different.

For the EMEP model, uncertainty due to model structure (diagnostic case) includes; ***but is not limited to:***

(1) Simplification of air chemistry - including, the question of linearity.

(2) Assumption of single vertical layer.

(3) Simplification of dry S deposition process.

(4) Simplification of wet S deposition process.

(5) Assumed immediate complete mixing of emissions into mixing layer.

(6) Omission of horizontal diffusion.

(7) Omission of vertical advection and related phenomena (e.g. frontal movements and deep convection).

(8) Omission of exchange between boundary layer and free atmosphere.

(9) Omission of shallow convection.

(10) Omission of orographic effects.

Model *parameter* uncertainty should also be the same for both diagnostic and forecasting cases unless the system changes. As an example of how the "system could change", let us assume that the SO_2 wet deposition rate, k_w, is currently oxidant-limited. In this case we should expect the uncertainty of k_w to change in the future if the background level of oxidant increases, i.e. such that k_w is no longer oxidant-limited. For the EMEP model, uncertainty will arise from the parameters listed in Table 2.1.

In comparison to parameter uncertainty, there is a clear difference between diagnostic and forecasting uncertainty for *forcing functions*. In the diagnostic case uncertainty arises from our *interpretation* of the actual forcing functions, i.e. either data is incomplete or we must transform it to make it compatible with the model. We can illustrate this point by considering the use of precipitation data as a forcing function of the EMEP model. The density of precipitation stations from which these data are derived is very crude compared to EMEP's spatial coverage. Consequently, these data must be interpolated before they can serve as input to the EMEP model. This "interpretation" is an example of diagnostic error due to the model's forcing functions. Other error of this nature arises from estimation of S emission and wind velocity fields.

On the other hand, the *forecasting* aspect of forcing function uncertainty refers to our inability to accurately forecast future forcing functions. In other words, we can only estimate the magnitude of future precipitation, S emissions and wind velocity. Interannual meteorologic variability and future climate change are part of this category of uncertainty. The sources of forcing function uncertainty in the EMEP model are summarized in Table 4.1.

There is also a difference between diagnostic and forecasting uncertainties related to *initial state uncertainty*. As with the forcing functions, uncertainty arises in the diagnostic case because we are unable to accurately translate actual boundary and initial conditions into our model, i.e. we cannot input the exact SO_2 and $SO_4^=$ boundary and initial concentrations into our model. The sources of possible initial state uncertainty are summarized in Table 4.2.

For the forecasting case, uncertainty arises because we are unable to exactly estimate the initial states at the beginning of the forecasting period.

Uncertainty due to the final category of uncertainty in the EMEP model, *model operation* includes: (1) input-output processing, (2) trajectory computations, and (3) solution of EMEP equations. One type of input-output processing error is the interpolation of input emissions' data. As an

Table 4.1. Forcing functions in the EMEP long-range transport model.

Symbol	Explanation	Unit
Q	Sulfur emissions	$kt\ yr^{-1}$
u,v	Components of the transport wind vector	$m\ s^{-1}$
p	Precipitation	$mm\ hr^{-1}$

Table 4.2. Initial State Uncertainties in EMEP Model.

Horizontal boundary conditions

Vertical boundary conditions

Initial conditions

example, emissions' input data are illustrated in Figure 4.4. During trajectory calculations, however, emissions' data are interpolated as in Figure 4.5 which causes some error in the input to equations (3.10) and (3.11)*.

Uncertainty in the trajectory calculations arises from the so-called *Petterssen method* described in Section 3.2.

Uncertainty due to solution of EMEP equations refers to the technique for solving equations (3.10) and (3.11).

Finally, we summarize the above uncertainties of the EMEP model in Table 4.3.

*In this example we call the transformation of actual sulfur emissions to the input data in Figure 4.4 *forcing function uncertainty*, and the interpolation of these input data by the model from Figure 4.4 to Figure 4.5 as *model operation uncertainty*. We term it *operation uncertainty* because it refers to an *internal* operation of a specific model.

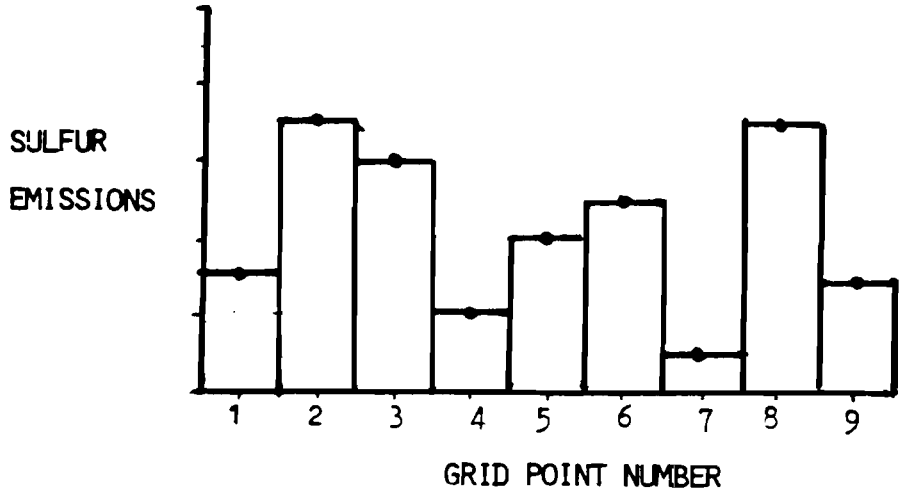

Figure 4.5. **Form of emission data which are input to the EMEP model.**

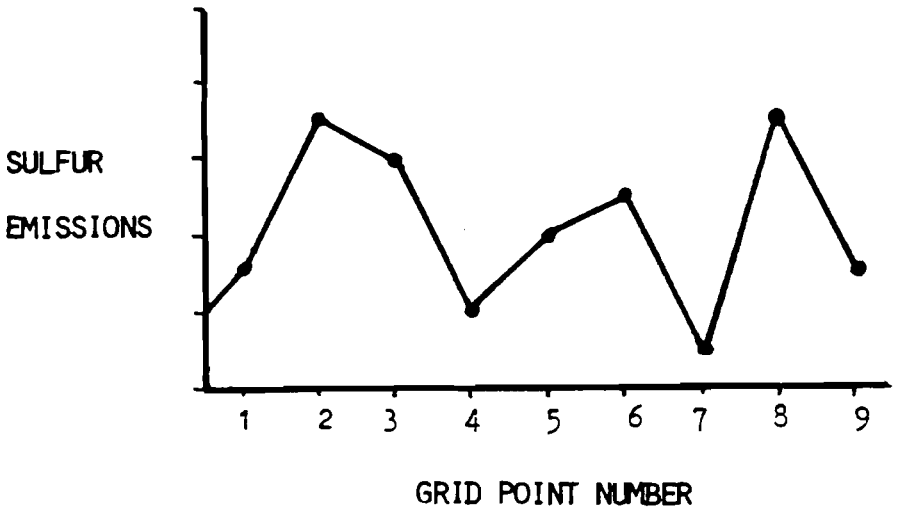

Figure 4.6. **Interpolation of emission data from Figure 4.5 for model computations.**

Table 4.3. A summary of some EMEP model uncertainties.

		DIAGNOSTIC UNCERTAINTY	FORECASTING UNCERTAINTY
1.	MODEL STRUCTURE	• As listed in section 4.2	• Changes in co-pollutant concentrations
2.	PARAMETERS	• Estimation errors of parameters in Table 3.1	• Changes in co-pollutant concentrations
3.	FORCING FUNCTIONS	• Estimate of current magnitude and spatial distribution of sulfur emissions	• Forecasted sulfur emissions
		• "Smoothing" errors and measurement errors of of precipitation	• Interannual meteorological variability (precipitation and wind patterns)
		• "Smoothing" errors and measurement errors of wind velocities	• Long term climate change
3.	INITIAL STATE	• Estimation and approximation errors:	• Future boundary and and initial conditions
		- boundary conditions - initial conditions	
4.	MODEL OPERATION	• Input/output processing	• Forecasting uncertainties same as Diagnostic uncertainties
		• Trajectory calculations for processing wind velocity data	

5. SCREENING AND RANKING OF UNCERTAINTY

The goal of this screening exercise is to limit the number of uncertainties which must be quantitatively evaluated in the next step of the uncertainty analysis. To do so we draw on sensitivity analyses conducted by EMEP and other investigators (cf. Eliassen and Saltbones, 1983 and Anon, 1983), as well as additional calculations, reviewed in a separate paper (Bartnicki and Alcamo, forthcoming).

As pointed out in Section 1.2, there are difficulties in translating results of sensitivity analysis to conclusions about uncertainty since sensitivity analysis and uncertainty analysis (as defined in this paper) have different goals. We therefore take a pragmatic approach, and rather than eliminate any uncertainties from further consideration, we assign them to categories of *first* and *second priority*. We will be conservative and assign to the second priority only those uncertainties where there is strong evidence that they are less important than other uncertainties. Remaining uncertainties are considered to have first priority. As will be seen, most uncertainties are placed in the first priority category, though further sensitivity analyses may permit us in the future to increase the number of "second priority" uncertainties.

Model Structure - The following uncertainties described in Section 4.2 are assigned to a lower priority: (1) Assumption of immediate complete mixing of emissions into mixing layer, (2) Omission of horizontal diffusion, and (3) Omission of shallow convection,

(1) There are physical reasons why the *assumption of immediate complete mixing* of *emissions into the mixing layer* would not add large

uncertainty to the EMEP calculations. During the day, especially with convective conditions, pollutants are mixed relatively quickly after emission. The characteristic time in which a parcel of pollutants rises to the top of mixing layer is less than one hour (Lamb, 1984), which is less than the computational time step. Therefore, the assumption of complete initial mixing of pollutants can be justified for daytime transport. During the night, although stable conditions usually inhibit vertical mixing, lateral mixing still occurs because of the different heights of emissions. Even if the above arguments are not strong enough to put this uncertainty into a lower priority, in practice this phenomenon is parameterized by coefficient α in equation (3.10), the local deposition coefficient. Consequently we take this ***model structure*** uncertainty into account by investigating the ***parameter*** uncertainty of α.

(2) The ***omission of horizontal diffusion*** is considered less important than other uncertainties because of the smaller scale effects of this diffusion compared to the scales treated by the EMEP model. Considering the large initial size assumed for a parcel of air pollutant in the EMEP model (150 x 150 x 1 km) we do not expect horizontal diffusion to affect the mixing of pollutants during the lifetime of a typical 96 hour trajectory. In support of this conclusion, Prahm and Christensen (1977), using an Eulerian one-layer model similar to the EMEP model, found small changes in computed SO_2 and $SO_4^=$ air concentrations (around 3%) when they compared models with and without horizontal diffusion.

(3) ***Shallow convection*** intensifies pollutant mixing within the mixing layer and also chemical transformation of pollutants. The first effect would influence the value of α in equation (3.10) and the second effect, k_t in the

same equation. We can take this uncertainty into account, therefore, by investigating the parameter uncertainty of α and k_t.

The remaining model structure uncertainties listed in section 4.2 are placed in the first priority category.

Model Parameters and Forcing Functions - All of these uncertainties are currently considered very important.

Initial State - Of the uncertainties of this type listed in Table 4.3, we may consider the uncertainty due to the ***vertical boundary condition*** to be contained in the the uncertainty of parameter b in equation (3.13). We can therefore transfer this type of ***initial state*** uncertainty to ***parameter*** uncertainty. Consequently "vertical boundary condition" as a separate uncertainty has been placed in a lower priority category.

Model Operation - Bartnicki et al. (forthcoming) present evidence that uncertainty due to the ***trajectory calculation method*** is relatively unimportant. They examined analytical versus numerical trajectories for an artificial rotational wind and found that after 96 hours of travel, trajectory positions differed by less than 15 km.

The sources of uncertainty currently assigned "Second Priority" are presented in Table 5.1. By default all other uncertainties have a higher priority.

Table 5.1. "Second Priority" Model Uncertainties

1. MODEL STRUCTURE

   - Assumption of immediate complete mixing of emissions into mixing layer.
   - Omission of horizontal diffusion.
   - Omission of shallow convection.

2. MODEL PARAMETERS - none

3. MODEL FORCING FUNCTIONS - none

4. INITIAL STATE

   - Vertical boundary condition.

5. MODEL OPERATION

   - Trajectory calculation method.

6. METHODS TO EVALUATE DIAGNOSTIC UNCERTAINTY

In this section we concentrate on the evaluation of diagnostic uncertainties assigned "first priority" after screening and ranking of Section 5. Unfortunately, a discussion of all important diagnostic uncertainties is outside the scope of this paper, though we try and highlight some of the more important sources.

6.1. Model Calibration/Verification

In Section 1.2 we reviewed the drawbacks to model calibration/verification in assessing model uncertainty. We also pointed out that model calibration/verification is necessary and useful though insufficient for this task. It is *necessary*, as noted earlier, because without data comparisons we have no standard with which to compare model output with reality. It is *useful* because the departure of model output from observations is a measure of the *magnitude* of model diagnostic uncertainty. The goodness of this measure naturally depends upon the amount of data and range of environmental conditions that the model is tested against. Since diagnostic uncertainty varies with environmental conditions as noted in Section 4.1, the more environmental conditions, i.e. data sets, the model is tested against, the closer we come to the "expected value" of diagnostic uncertainty. Using the EMEP model as an example, a single comparison of annual average model output with observations provides only one value of model uncertainty under specific environmental conditions. This comparison does, however, give us an idea of the possible maximum diagnostic uncertainty.

6.1.1. Interpretation of Model Calibration/Verification

There is no straightforward way to translate the results of model calibration and verification into estimates of ε, model uncertainty. In Figure 6.1 we illustrate three possible ways in which model calibration and verification can be combined in modeling practice. In Case I, model parameters are adjusted so that model output agrees with Data Set A ("calibration"). Using these calibrated parameters and new forcing functions, model output is compared to Data Set B ("verification"). We denote the departure of model output from observations as ε_{1a} and ε_{1b}, respectively. In Case II, the model parameters are again adjusted so that model output agrees with Data Set A. This exercise is repeated with new forcing functions so that model output also agrees with Data Set B. We have therefore "calibrated" the model separately to two independent data sets and obtain two independent parameter sets. In Case III, we are interested in finding the single parameter set which fits both Data Sets A and B simultaneously. In other words, this process yields a single parameter set for the two data sets.

In general, given an identical model and an identical calibration procedure for all cases, we expect

$$\varepsilon_{1a} = \varepsilon_{2a} \approx \varepsilon_{2b} < \varepsilon_{3a} \approx \varepsilon_{3b} < \varepsilon_{1b} \tag{6.1}$$

Each epsilon is an estimate of *diagnostic uncertainty* since we assume our forcing functions and initial states are input to the model. Individually they are not necessarily good estimates of *average* diagnostic uncertainty. Even though ε_{2a} and ε_{2b} from Case II are smaller than ε_{3a} and ε_{3b} from Case III, uncertainty was "conserved", i.e. "apparent" diagnostic uncertainty has decreased but we have increased forecasting uncertainty

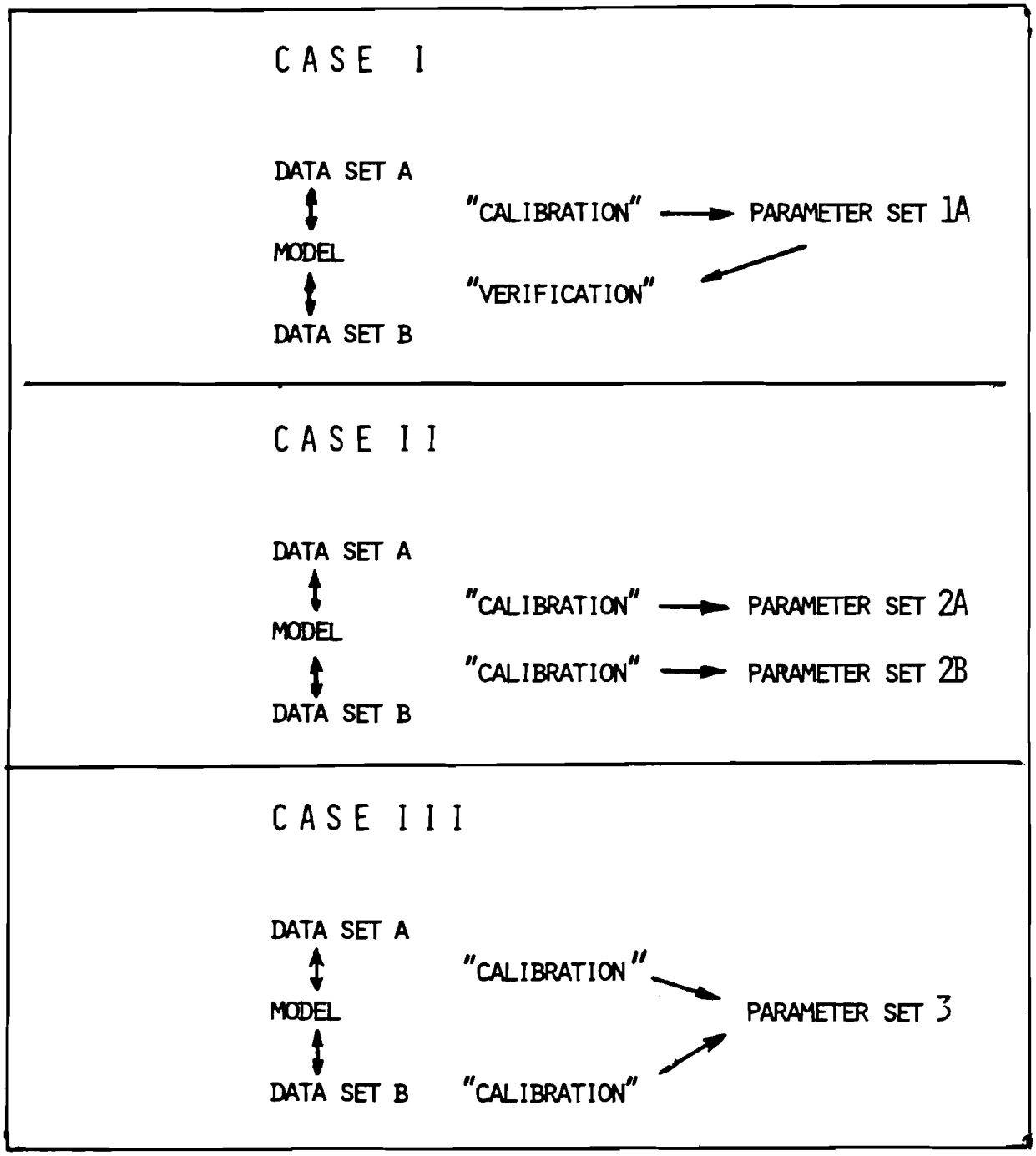

Figure 6.1. **Three ways of combining model calibration and verification.**

because we do not know which of the two parameter sets in Case II to use for forecasting.

In conclusion, caution must be used in interpreting comparisons of model output with observations.

6.1.2. Data Observations and Uncertainty Estimates

Later in this section we describe how to obtain quantitative uncertainty estimates of the EMEP model. The simplest check of these uncertainty estimates would be, of course simply to compare the observations with the computed frequency distribution. In the hypothetical example in Figure 6.2a we compare observed annual SO_2 air concentration with the frequency distribution of computed SO_2. We expect, for example, that 90% of the time an observation such as this would fall within the frequency distribution's 90% confidence interval. Though a single comparison of this nature proves little, a comparison of observations versus computed frequency distributions at *five* stations would serve as a check on our procedure for analyzing diagnostic model uncertainty. (This of course also depends on the accuracy of the data.) In fact, the probability that all five observations are outside the 90% confidence intervals of the frequency distributions is $(0.1)^5 = 0.001$ %. The probability of two or more being outside the 90% confidence interval is 1%. This serves as a way to check our procedure with data.

6.2. Model Structure

There is only one satisfactory way to evaluate this uncertainty and that is of course to compare different model structures. If alternative models are available then these comparisons can be performed with identical input

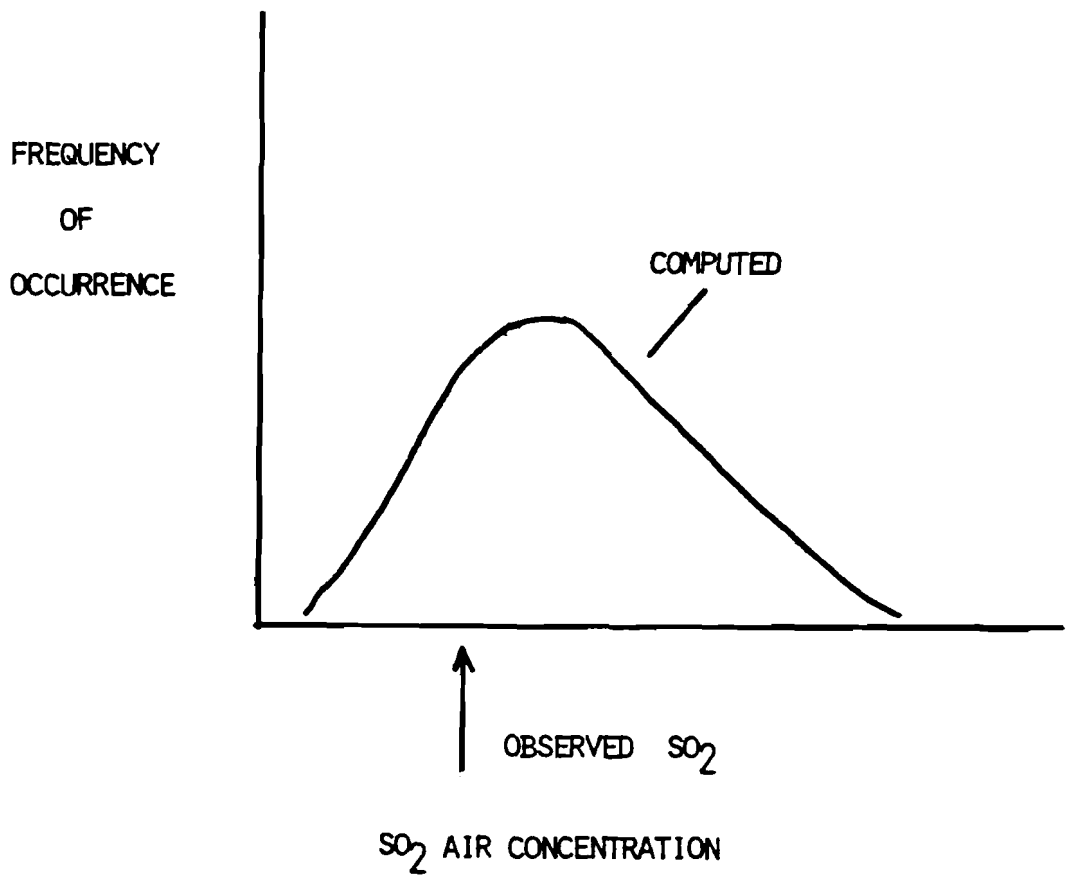

Figure 6.2a. Hypothetical comparison of observation with computed frequency distribution of SO_2 air concentration.

data (cf. MOI, 1982). If alternative models are not available, then certain mathematical terms which reflect key questions about model structure can be changed and comparisons made between original and revised model equations. A proposal for such a revision regarding non-linearity is given in the following section.

Recall, however, from Section 4.1 that these model experiments will yield the difference between *mean* calculations of different model structures. Even if the two model structures have an identical set of parameters and parameter values, initial states, etc. it is likely that the ε of the output uncertainty will be different for the two model structures. This idea is illustrated in Figure 4.2.

We should also note that uncertainty of model structure is sometimes expressed as uncertainty of parameters. For example, since k_t is known to be a "lumped parameter" related to complex atmospheric sulfur chemistry, it is not "observable" and we are therefore unsure of its values. In more complicated models there is a more detailed description of this chemistry and hence there will be a better chance that the new model's oxidation parameters will be observable, and therefore, better known.

6.2.1. The Linearity Question

The current configuration of variables in the EMEP model (equations 3.10 and 3.11) results in a proportional or "linear" relationship between sulfur deposition and air concentration and sulfur emissions. However the parameters in these equations are admittedly simplifications of much more complicated processes which occur in the atmosphere. The key "linearity" question is not whether these processes are non-linear, since to a certain

extent they are.* Instead it is whether they result in a *significant* departure from the implicit proportional relationship between a sulfur source and its deposition at another location. There are two reasons why this is a critical question for those interested in using the EMEP model for assessment of control scenarios. First, the linearity assumption permits us to superimpose the contributions from different sources together which allows us to examine the expected benefits of reducing sulfur emissions in a particular country independent of other countries. Otherwise we would have to take all sources and co-pollutants simultaneously into account. Second, by assuming linearity we can further assume that if we reduce the amount of sulfur emitted it will result in a proportional reduction of sulfur deposited. This linearity assumption was expressed as a straight line in Figure 3.1.

The linearity question in the decision context introduced in Section 3 of this paper is whether there is a linear relationship between source country i and receptor element j.

In order to answer this question we recall that the source receptor matrix between country i and receptor j depends mainly on:

1. synoptic scale atmospheric transport - i.e. wind velocity and deposition.
2. micrometeorology and dry deposition processes.
3. precipitation and wet deposition processes.
4. atmospheric chemistry.

*A description of relevant sulfur chemistry is outside the scope of this paper. The reader is referred to U.S. National Research Council (1983) for a good overview.

Since non-linearities occur mainly in numbers 3 and 4, our task then is to evaluate the importance of non-linear chemical factors relative to these other factors.

OTA (1984) and the U.S. National Research Council (1983) approach this task by using non-linear chemical models which represent some of the complex non-linear chemical mechanisms. In these model experiments a hypothetical parcel of air is followed for a period of days. Factors (1), (2), and (3) are included in the calculations in only a rudimentary fashion. As the U.S. National Research Council pointed out, conclusions deduced from these models are very sensitive to the modeler's assumptions of chemical pathways. Nevertheless, as knowledge of atmospheric chemistry improves, these models will give increasingly valuable insight to the linearity question.

EMEP investigators (Anon, 1983) added a non-linear term to the basic equations of the EMEP model to explore the effect of non-linearity. Oppenheimer et al. (1985) and Granat (1978) reviewed the data from Western U.S. and Northern Europe, respectively. A drawback to this data analysis is that it can only treat wet sulfur deposition, not total sulfur deposition, though most non-linearities are thought to occur in the wet phase rather than the dry phase.

Unfortunately a review of this previous work is outside the scope of this paper.

6.2.2. Non-linear Coefficients

One way to approach the linearity question is to *non-linearize* the coefficients in the EMEP model which represent possible non-linear atmospheric processes, i.e. we would treat the wet deposition rate (k_w), the SO_2 transformation rate (k_t) and the $SO_4^=$ removal rate (κ) as non-linear parameters rather than as constants. As an example, we could assign k_w the non-linear relation to SO_2 air concentration illustrated in Figure 6.2b. The basis of this relationship would be expert opinion. We would then investigate how much the *overall* relationship between sulfur emissions in country i and deposition or air concentration in receptor j departs from linearity due to these non-linear parameters. Since the relationship in Figure 6.2b is non-linear we would have to assign "background" SO_2 and $SO_4^=$ air concentrations along the trajectory paths from country i to receptor j. This is a disadvantage of the method. Advantages include: (1) The linearity question would be investigated in the same time and space scales as presented in Section 3. This means that we could compare in a consistent fashion the uncertainty of non-linearity with other uncertainties, such as the parameter and forcing function uncertainties discussed in the next section of this paper; (2) Experts could prescribe any number of different non-linear relationships of the type illustrated in Figure 6.2b. Therefore, this method provides a convenient opportunity to compare the views of different experts regarding non-linearity; (3) The method is relatively easy to perform.

The procedure would be as follows:

(i) Assign non-linear relationships to k_w, k_t, and κ.

(ii) Select country i, receptor j.

(iii) Assign background SO_2 and $SO_4^=$ air concentrations.

(iv) Solve EMEP equations for one year and for a unit sulfur emissions from country i to receptor j.

(v) Repeat (iv) for different levels of background SO_2 and $SO_4^=$ air concentrations.

From this analysis we obtain an estimate of uncertainty of computed sulfur deposition (or air concentration) at receptor j which accounts for a unit sulfur emissions from country i, non-linear relationships from (i), and a range of background SO_2 and $SO_4^=$ levels specified in (v).

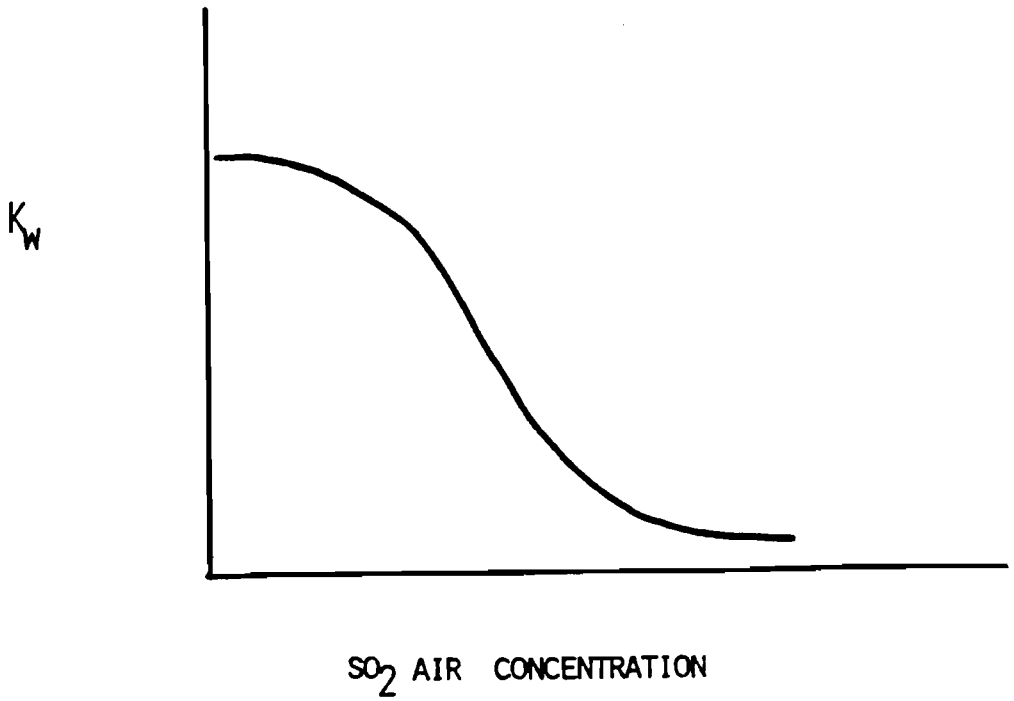

Figure 6.2b. Hypothetical relationship between k_w and SO_2 air concentration.

6.3 Monte Carlo Analysis of Composite Uncertainty (Parameter, Forcing Function, Initial State)

6.3.1. Overview

Monte Carlo Analysis provides a general and flexible approach to examining the combined uncertainties due to parameters, forcing functions and initial state errors. To illustrate how we apply this method recall the general model presented in Section 1:

$$\mathbf{Y} = \hat{\mathbf{G}}(\mathbf{X}) \tag{6.2}$$

For the EMEP model:

$$\mathbf{Y} = (c_1, c_2, d_w, d_d, d_t)$$
$$\mathbf{X} = (\beta_1 \cdots \beta_m, \varphi_1(x,t) \cdots \varphi_1(x,t))$$

where

c_1, c_2, d_w, d_d, d_t = EMEP state variables: SO_2 air concentration, $SO_4^=$ air concentration, wet deposition, dry deposition total deposition.

$\beta_1 \cdots \beta_m$ = parameters defined in Table 3.1

$\varphi_1(x,t) \ldots \varphi_n(x,t)$ = forcing functions: sulfur emissions, wind velocities, and precipitation

Using random numbers $\nu_{1\ldots m}$, $\mu_{1\ldots n} \in [0,1]$ we sample from the cumulative frequency distributions $F(\beta)$ and $F(\varphi)$ and obtain a β^t and φ^t such that $F(\beta^t) = \nu^t$ and $F(\varphi^t) = \mu^t$. In this analysis we have neglected all initial state uncertainties for the time being except for the vertical boundary condition which is represented by b. in equation (3.13). In this analysis we treat this boundary condition as a parameter.

Each β^i and φ^i is used to compute $\mathbf{Y} = (c_1, c_2, \ldots)$ by equations (3.10) through (3.14). An individual computation of $\mathbf{Y}$ is called a "realization" of $\mathbf{Y}$. We repeat this sampling and computation N times, until a statistically significant sample of ν and μ is drawn. We then compute the frequency distribution $f(\mathbf{Y})$from the set of realizations of $\mathbf{Y}$. The frequency distribution $f(\mathbf{Y})$ indicates the uncertainty of the state variables due to uncertainty reflected in $F(\beta_1), \ldots, F(\beta_m)$ and $F(\varphi_1), \ldots, F(\varphi_n)$.

6.3.2. Frequency Distribution of Forcing Functions

The forcing functions ($\varphi(x,t)$) of the EMEP model include winds, precipitation and sulfur emissions. In this section we present a method for assigning frequency distributions for wind velocity inputs to the model.

First we take the general form of the velocity vector $\bar{V}_i = (u_i, v_i)$ and transform it into a magnitude $|\bar{V}_i|$ and directional angle α_i.

Second we divide winds into 10 "transport wind" classes such that:

$$|\bar{V}_i| = (1 - \frac{i}{10})|\bar{V}_0| \tag{6.3}$$

and

$$\alpha_i = \alpha_0 + 2_i, \qquad i = 1,\ldots,10 \tag{6.4}$$

where

$|\bar{V}_i|$ = magnitude of transformed wind

i = number of "transport wind" class

$|\bar{V}_0|$ = magnitude of original wind

α_0 = angle of original wind

α_i = angle of transformed wind

2_i = angle changed by 2° increments.

Using the Peterssen method described in Section 3.2.1, we compute the trajectories between the source and receptor of interest according to the ten classes of $|\bar{V}_i|$ and α_i. This yields ten sets of trajectories $\{T_i\}$.

Finally we construct $f\{T_i\}$ by assigning probabilities to the occurrence of each of the 10 trajectory sets (Figure 6.3).

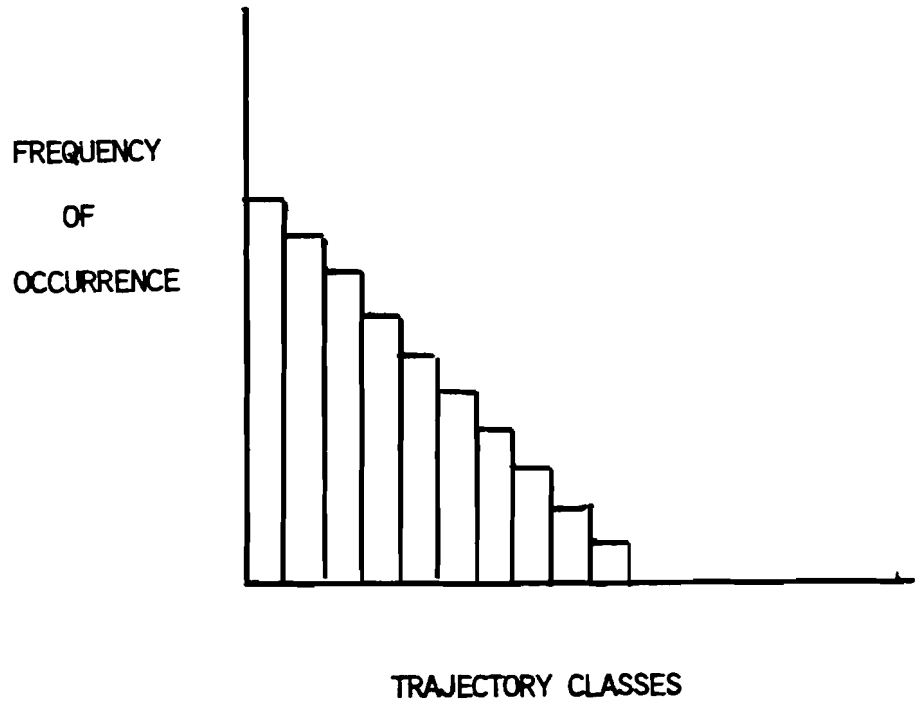

Figure 6.3. Hypothetical frequency distribution of trajectory classes.

6.3.3. Frequency Distribution of Parameters

A critical exercise in using Monte Carlo Analysis is to intelligently select the frequency distribution of parameters. Interpretation of these frequency distributions becomes a key issue because through their selection we express our *a priori* uncertainty about these variables. An important question is, what is the least biased way for an analyst to express

his/her uncertainty in a parameter frequency distribution? First, we recall that the EMEP model parameters (Table 3.1) are mostly "lumped" parameters, i.e. they reflect a conglomeration of processes occurring in nature and averaged broadly in time and space. The particular parameter values used in the model are very unlikely to be observed at any single time or location in Europe, though it may in fact be an excellent average for all of Europe over an entire year. For example, it is well known that k_t varies according to sunlight intensity, temperature, amount of co-pollutants, humidity and other factors and therefore fluctuates according to time of day, season, etc. It is rather unlikely that any single literature value of k_t will coincide with the European lumped average. Also it is unlikely that the exact shape of the frequency distribution for any of the parameters listed in Table 3.1 will be known. Under these circumstances, we assume that the parameter frequency distribution is a triangular distribution with a median equal to the EMEP parameter value and extremes from the literature or experts.

Another possible starting assumption is that parameters have a rectangular or uniform frequency distribution. However this makes the unlikely assumption that all values between the extremes are as equally likely to occur. As explained above, this is not necessarily a good assumption. However it does give the analyst an idea of what effect a conservative estimate of parameter uncertainty will have on model output.

6.3.4. An Algorithm for Composite Uncertainty

In practice the Monte Carlo analysis of combined uncertainty would be conducted in the following steps:

(i) Sample f{T}, i.e. using a random number, select a set of trajectories from the frequency distribution f{T}.

(ii) Sample $f(\beta)$, $f(\varphi(x,t))$

(iii) Compute $\mathbf{Y}(\cdot)$ by equations (3.10) through (3.15) and store.

(iv) Repeat (i) → (iii) **N** times, i.e. until a statistically significant sample of {T}, β and $\varphi(x,t)$ are drawn.

(v) Compute frequency distribution $f(\mathbf{Y})$.

6.3.5. An Example

In order to illustrate the above method we have made some *a priori* assumptions about frequency distributions of four of the parameters in the EMEP model. First, we have assumed that they represent the frequency of occurrence of particular annual and European average values. Second, we have assumed that they are triangular-shaped with EMEP parameter values as the median, and extremes based on the literature and expert opinion. As a result we have selected the distributions in Figure 6.4.

We examine how EMEP state variables are affected by the assumed frequency distributions of the four parameters in a case study of U.K. sulfur emissions and Southern Sweden sulfur deposition. This is only the first of five case studies. The source-receptor combinations which have not yet been analyzed are: Netherlands - Northern Denmark, Czechoslovakia - Northern GDR, FRG - Southern Poland, Poland - Central Hungary. These combinations were selected to cover a wide range of geographic and meteorologic conditions. In this analysis we use 1980 meteorological inputs and are interested in an annual time scale.

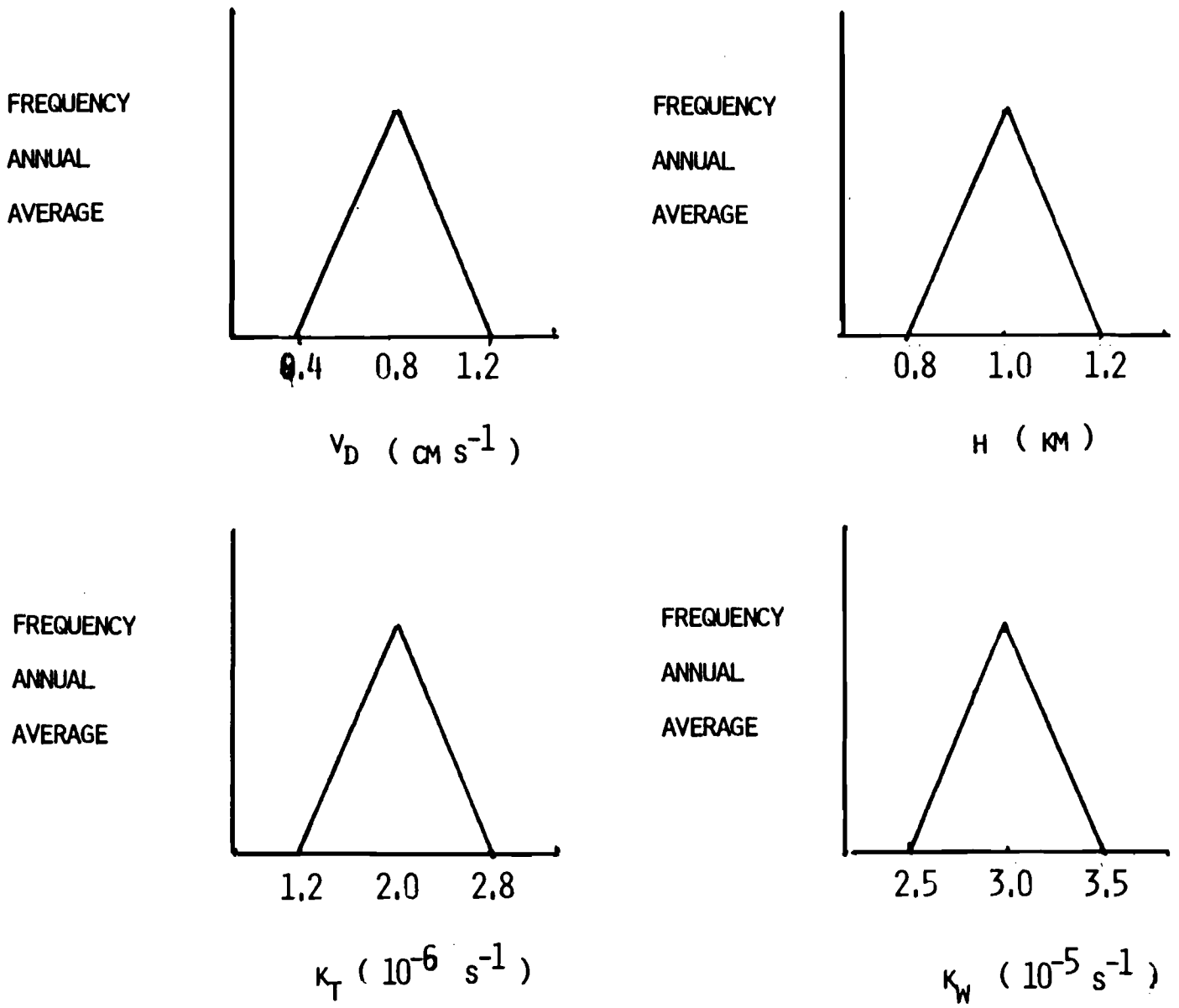

Figure 6.4. Assigned frequency distributions of v_d, h, k_t and k_w.

Figures 6.5 through 6.9 presents the resulting frequency distributions of SO_2 (air), $SO_4^=$ (air), dry sulfur deposition, wet sulfur deposition, and total sulfur deposition. For example, Figure 6.5 reflects the uncertainty in computed annual average SO_2 air concentration in an EMEP grid element in Southern Sweden (resulting from U.K. emissions) due to uncertainty of v_d, h, k_t, and k_w. The coefficient of variation (c.v. = $\sigma/\bar{x}$ where σ = standard deviation and $\bar{x}$ = mean) of these distributions are reported in Table 6.1. Note that the largest c.v. occurs for SO_2 air concentration (0.27) and the smallest for dry and total sulfur deposition (0.09). This reflects the integrative nature of sulfur deposition in the EMEP model. For all forms of deposition the c.v. is rather small (around 0.1 or 10%) suggesting that the uncertainty in computed deposition due to uncertainty of these four parameters is rather small. But this conclusion depends on the *a priori* acceptance of the model structure and confidence that the uncertainty of these parameters is truly reflected in the frequency distributions of Figure 6.4. Also this method has so far been applied only to the U.K. - Southern Sweden case.

Table 6.2 presents the c.v. for SO_2 air concentration and total sulfur deposition as it is affected by the uncertainty of each of the four parameters individually. Note that v_d has the largest effect on uncertainty of SO_2 air concentration (c.v. = 0.23) yet a small effect on total sulfur deposition (c.v. = 0.02). An examination of the EMEP equations can explain this compensation, though the question remains whether nature behaves in the same manner.

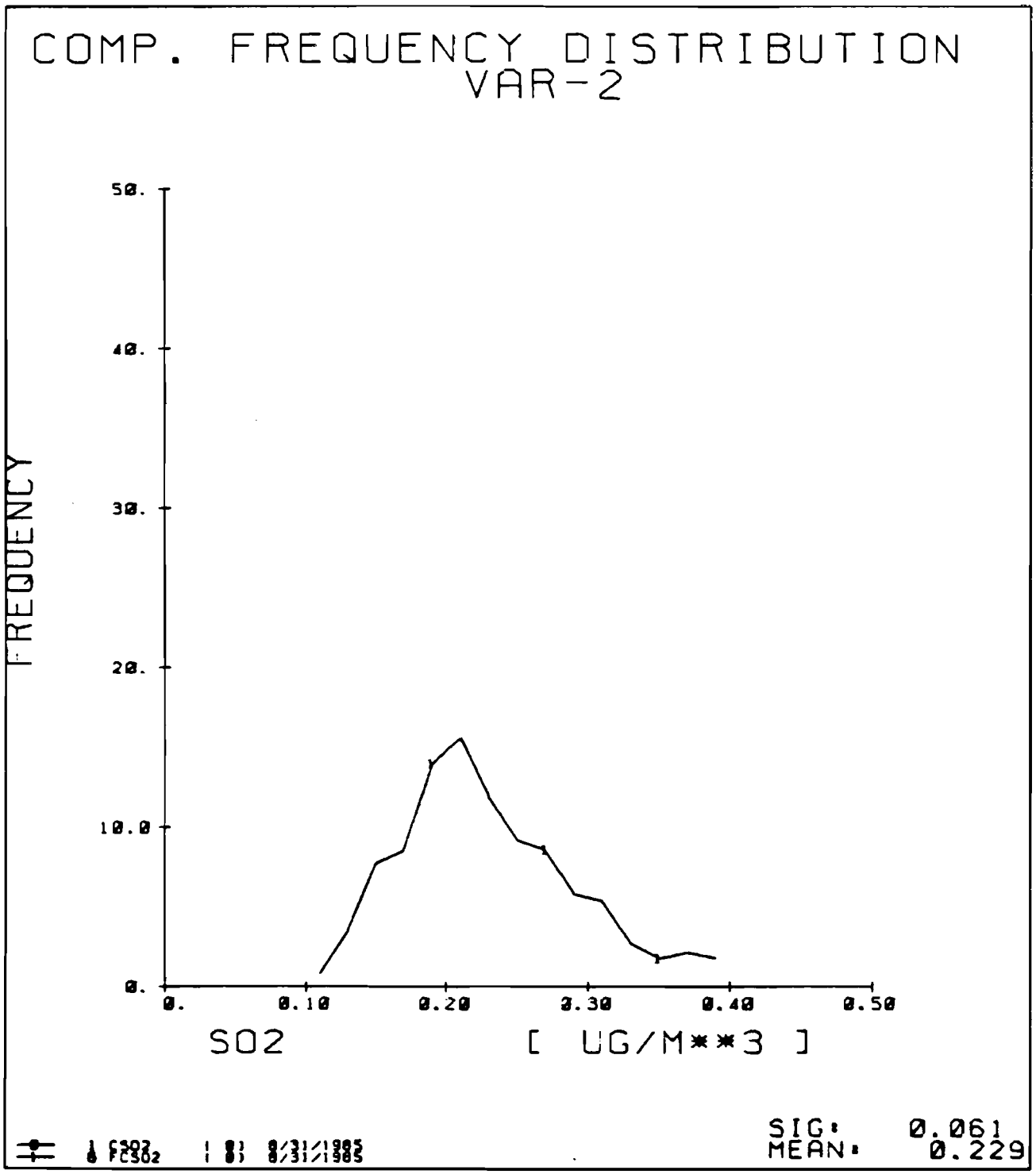

Figure 6.5. Computed frequency distribution of SO_2 (air)

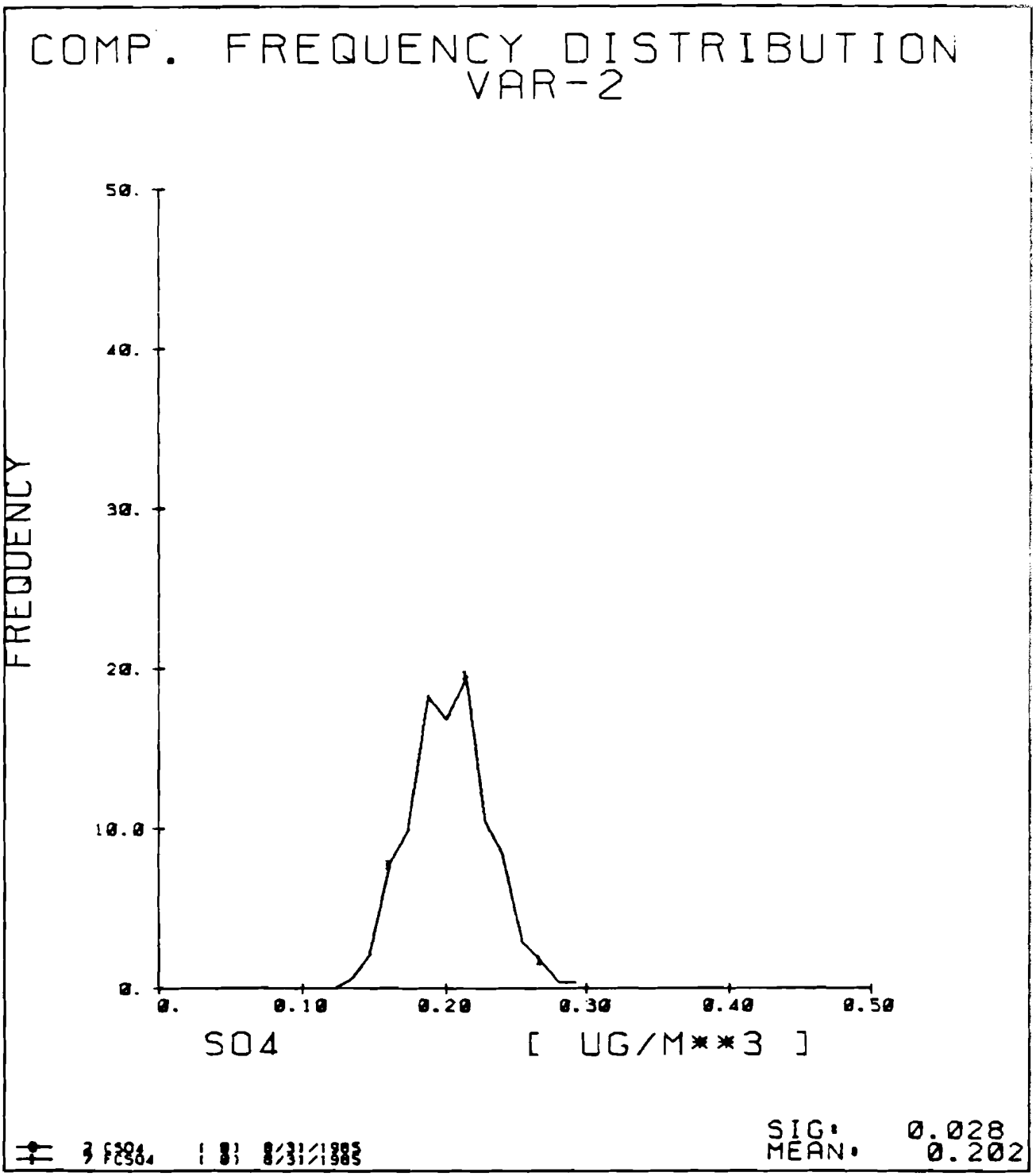

Figure 6.6. **Computed frequency distribution $SO_4^=$ (air).**

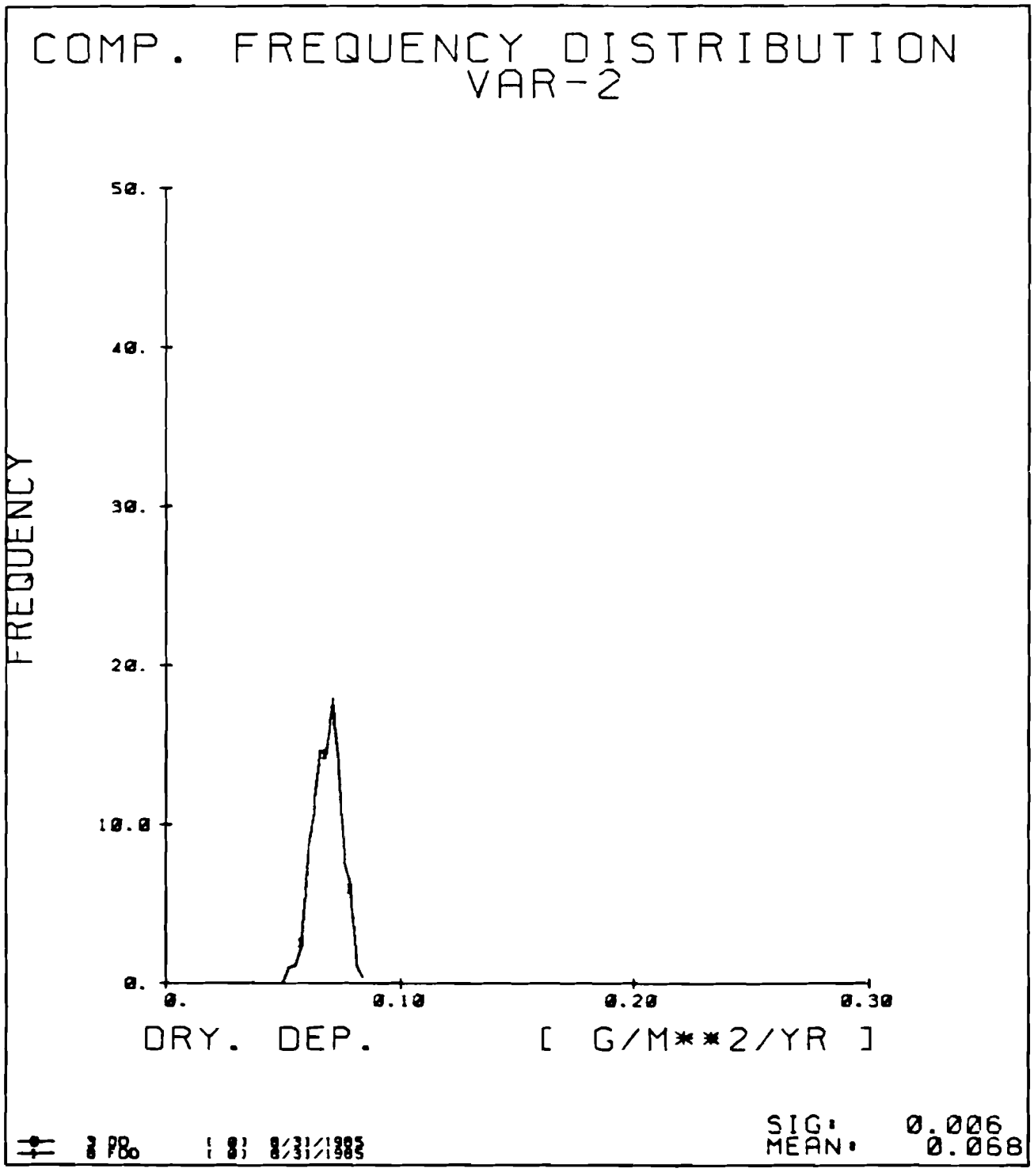

Figure 6.7. **Computed frequency distribution dry sulfur deposition.**

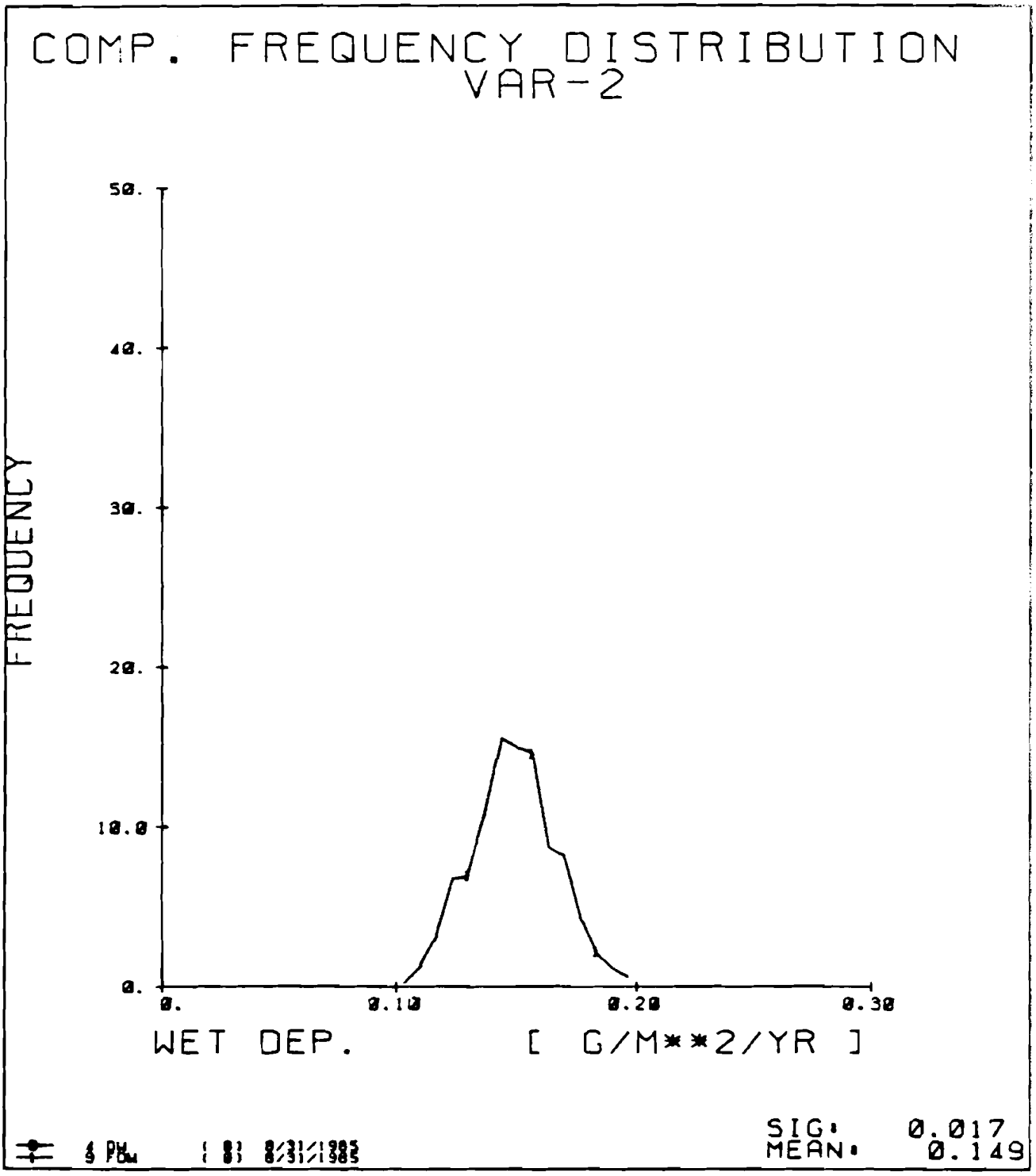

Figure 6.8. **Computed frequency distribution wet sulfur deposition.**

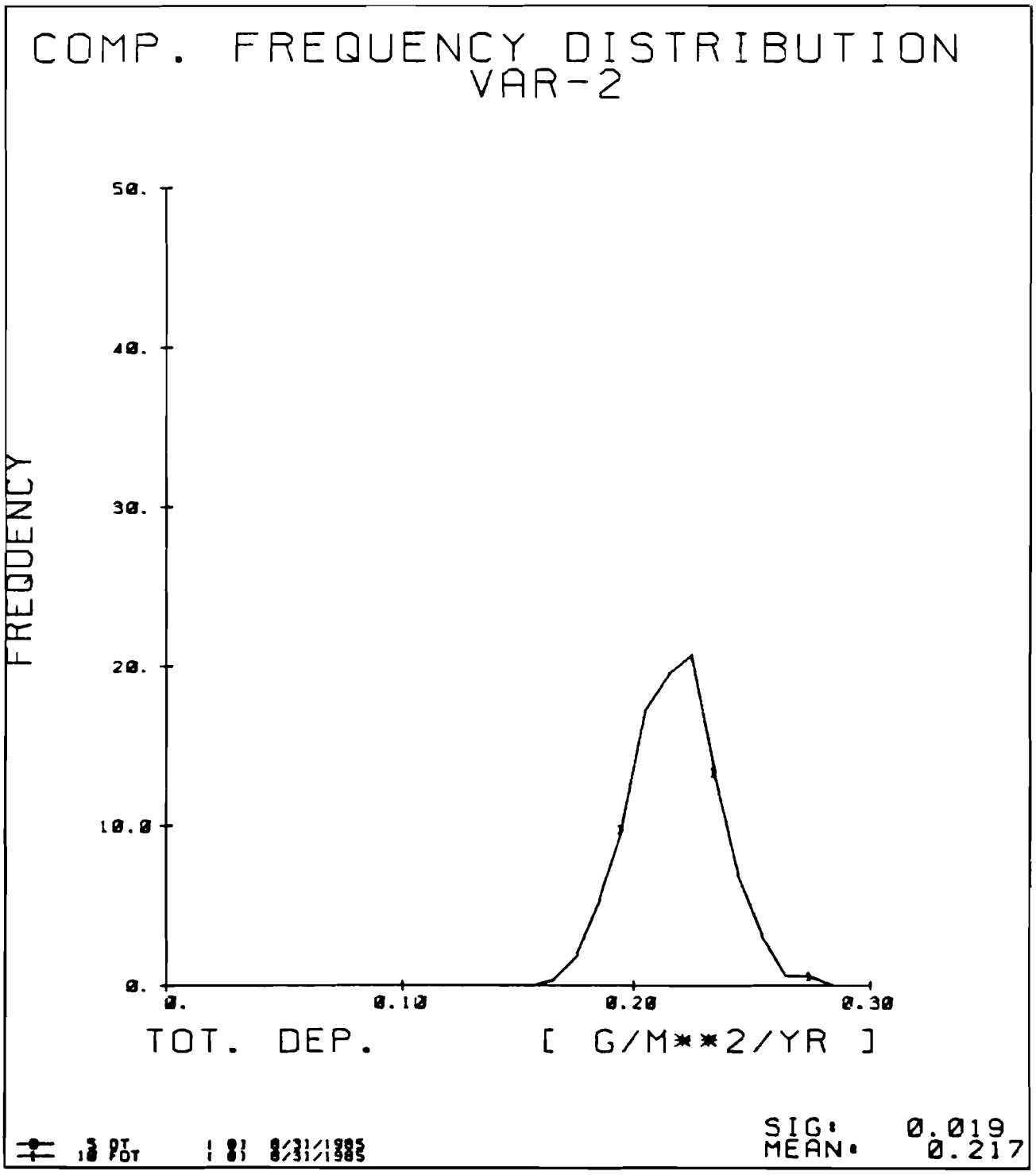

Figure 6.9. **Computed frequency distribution total sulfur deposition.**

Table 6.1. Influence of Simultaneous Uncertainty of 4 Parameters (v_d, h, k_t, k_w) on EMEP State Variables

State Variables	Coefficient of Variation
SO_2(air)	0.27
$SO_4^=$ (air)	0.14
Dry Sulfur Deposition	0.09
Wet Sulfur Deposition	0.11
Total Sulfur Deposition	0.09

Table 6.2. Influence of Individual Parameter Uncertainty on EMEP State Variables

Parameter Varied	Coefficient of Variation	
	SO_2 (air)	Total Sulfur Deposition
v_d	0.23	0.02
h	0.09	0.04
k_t	0.04	0.06
k_w	0.04	0.02
v_d, h, k_t, k_w,	0.27	0.09

6.4. Future Work

Section 6 presents some preliminary work in evaluating EMEP diagnostic model uncertainty. Future tasks concerning composite uncertainty will include:

(i) Refinement of probability encoding techniques to systematically translate expert opinion into parameter and forcing function frequency distributions.

(ii) Analysis of combined parameter, forcing function and initial state uncertainties by using the Monte Carlo algorithm presented in this section.

(iii) Application of composite uncertainty analysis to at least five source-receptor combinations in Europe.

(iv) Development of algorithms to take into account co-variance between different parameters and forcing functions.

(v) Experimentation with a wide variety of different forms of frequency distributions (e.g. triangular, rectangular, etc.) for parameter and forcing function frequency distributions.

(vi) Comparison of observations with uncertainty estimates of SO_2 and $SO_4^=$ air concentrations and wet sulfur deposition.

Future tasks concerning ***model structure*** will involve:

(i) Model experiments concerning linearity described in this section.

(ii) Comparison of results from different European long-range transport models.

(iii) **Further analysis of model structure uncertainties identified in** Section 4.2.

7. METHODS TO EVALUATE FORECASTING UNCERTAINTY

In this section, as in the last section, we emphasize those uncertainties which are considered of higher priority after the screening and ranking exercise of Section 5. Full consideration of these uncertainties, is however, outside of this paper's scope.

7.1. Model Structure: The Linearity Question

In Section 6.2 we formulated the so-called "linearity question" in terms of the decision making context of the EMEP model. Even though data analysis or model experiments indicate that there is *currently* a linear relationship between sulfur emissions and deposition it is still possible that their relationship will not be linear under future atmospheric conditions. Put in another way, under current levels of sulfur co-pollutants, e.g. NO_x, H_2O_2, O_3, we might expect that SO_2 oxidizes to $SO_4^=$ at such a rate that the relationship between sulfur emissions to deposition is apparently linear. However, the question remains whether this relationship will continue to be linear if the molar ratio of SO_2 and its co-pollutants significantly changes in the future. It is possible that this molar ratio can change if, say, power plant emissions are controlled but not vehicular emissions. We conclude, therefore, that the linearity question has a "forecasting" as well as a "diagnostic" component.

One way to approach this problem would be to assume wider ranges for the non-linear function of wet deposition rate (k_w) presented in Figure 6.2b. In addition we may wish to assume the SO_2 transformation rate (k_t) also has a larger uncertainty due to the effect of co-pollutants.

7.2. Forcing Functions: Interannual Meteorological Variability

This uncertainty arises from our inability to anticipate future sulfur emissions and meteorological variables such as wind velocities and precipitation. If we assume that the EMEP model will be used to forecast the results of changing sulfur emissions then we may also assume that these sulfur emissions will be given. Consequently, in this paper we do not address sulfur emissions' uncertainty. Meteorological variability cannot be so easily neglected. We can make two alternative assumptions to analyze this uncertainty:

(1) That future interannual meteorological variability will be affected by global climate change brought on by, say, increasing tropospheric concentrations of CO_2 and other trace gases; the "Climate Change" approach;

(2) That future interannual meteorological variability will resemble past variability; the "Past Variability" approach.

7.2.1. "Climate Change" Approach

Analysis of interannual meteorological variability could involve use of global general circulation models (GCM) from which we could derive new precipitation and wind patterns for Europe consistent with scenarios of global climate change. These patterns could then be used in the EMEP model to generate new source-receptor relationships. To use GCMs for this purpose we must first determine:

(1) Will the temporal and spatial resolution of the GCM be appropriate for running the EMEP model?

(2) Does the scientific community have sufficient confidence in particular GCMs to allow their use in this kind of analysis?

(3) What scenarios of climate change should be investigated?

(4) How can interannual variability be derived from these scenarios of climate change?

An alternative approach is being used within the IIASA Acid Rain Project by Pitovranov (forthcoming). This involves:

(i) Correlating historical hemispheric temperatures with long term precipitation data at several European stations.

(ii) Using (i) to estimate future precipitation changes at these stations for various scenarios of future hemispheric temperature changes. (These future temperature scenarios can be taken, for example, from current work on assessing the impact of increased CO_2 and trace gas concentrations in the atmosphere.)

(iii) Using revised precipitation values from (ii) as new input forcing functions for the EMEP model and recomputing sulfur deposition.

7.2.2. "Past Variability" Approach

The simplest version of the "Past Variability" approach is utilize results from multi-year runs of the EMEP model. Since the only inputs which were varied from year to year were meteorological inputs, differences between computed sulfur deposition should reflect interannual meteorological variability. The following summarizes a statistical analysis conducted on 4 source-receptor matrices covering the annual periods in Table 7.1.

Table 7.1. Time periods for EMEP source-receptor matrices.

October 1978	-	September 1979
October 1979	-	September 1980
October 1980	-	September 1981
October 1981	-	September 1982

(i) Since the effect of interannual meteorological variability will depend on the geographic pattern of sulfur emissions, we selected 3 scenarios computed by the IIASA RAINS model (see for example, Hordijk, 1985 and Alcamo et al., 1985). These scenarios were selected because of their large spatial variability and are noted in Table 7.2.

(ii) Each of the four unit-source-receptor matrices is multiplied by each of the three sulfur emission scenarios. This yields four sulfur deposition matrices for each sulfur emission scenario.

(iii) The four deposition matrices produced by each sulfur emission scenario are compared on a grid element by grid element basis with the 4-year *mean* deposition matrix. The following statistics were used for this comparison:

root mean square (*rms*) $= \frac{1}{N}\sqrt{\sum (a_{mn} - b_{mn})^2}$

absolute deviation (*ad*) $= |a_{mn} - b_{mn}|$

mean absolute deviation(*mad*) $= \frac{1}{N}\sum |a_{mn} - b_{mn}|$

relative deviation (*rd*) $= \left|\frac{a_{mn} - b_{mn}}{a_{mn}}\right|$

mean relative deviation (*mrd*) $= \frac{1}{N}\sum \left|\frac{a_{mn} - b_{mn}}{a_{mn}}\right|$

where

a_{mn} = grid element of the 4-year mean deposition matrix (October 1978 - September 1982)

b_{mn} = grid element of the comparison matrix (from periods listed in Table 6.1)

N = # grid elements

Table 7.3 summarizes the computed root mean square error (*rms*) for the four annual deposition matrices compared to the four-year mean. In this case the *rms* indicates which computed deposition matrix has the largest variability from the four-year mean on an aggregated basis, i.e. which matrix year has the "largest" interannual meteorologic variability. Note that the *rms* depends on the sulfur emission scenario, not only the meteorologic input data. This suggests that in order to choose the "most meteorologically variable" year we must also be able to estimate the sulfur emission pattern.

Table 7.2. Sulfur Emission Scenarios.

Country	1980	2010 Ref. Scenario. kt/yr	2010 Major Poll Controls kt/yr
Albania	54.4	50.1	14.9
Austria	208.9	185.9	101.0
Belgium	543.8	429.7	244.0
Bulgaria	590.6	853.2	196.0
Czechoslovakia	1723.5	1353.1	359.3
Denmark	329.3	211.2	148.4
Finland	327.3	260.9	193.7
France	1387.5	769.1	447.0
FRG	2060.9	1498.4	658.7
GDR	2427.2	2041.4	758.6
GB	1254.7	188.1	72.4
Hungary	772.4	745.8	189.3
Ireland	137.0	170.4	48.8
Italy	1510.0	1449.4	516.2
Luxembourg	41.4	36.9	7.8
Netherlands	455.3	703.4	324.8
Norway	94.9	90.9	56.1
Poland	2447.7	2042.2	633.9
Portugal	63.9	49.8	21.2
Romania	624.5	916.2	272.3
Spain	1155.9	1085.5	311.8
Sweden	347.9	266.5	171.6
Switzerland	69.6	53.4	25.6
Turkey	382.0	215.8	86.4
UK	2118.6	1487.5	719.3
USSR	10125.4	7392.9	2462.4
Yugoslavia	1374.3	1294.0	348.6
Total	31629.0	25842.0	9390.0

The computed mean absolute deviation (*mad*) is summarized in Table 7.4 which presents *mad* for the grid elements of three countries and all Europe. (The countries shown are the last three in an alphabetical order of the 27 largest European countries in Europe.) Results for two of the three sulfur emission scenarios are shown. The absolute deviation, of course, strongly depends on the amount of sulfur emitted. The difference in absolute

Table 7.3. Summary of computed root mean square error.

Scenario	European Emissions (kt/yr)	Root Mean Square Error ($g\ m^{-2}\ yr^{-1}$) Matrix: 7879	7980	8081	8182
Yr 1980	31629	.208	.188	.174	.201
Yr 2010 Reference	25842	.183	.170	.157	.183
Yr 2010 Major Poll Controls	9390	.077	.080	.072	.102

deviation between the two sulfur emission scenarios shown in this table (a factor of 2 to 3) reflects the difference in total sulfur emissions of the two scenarios.

The mean relative deviation (*mrd*) is summarized in Table 7.4. As expected, the mean relative deviation is relatively independent on the geographic pattern of sulfur emissions. The mean relative deviation for all grid elements in Europe is approximately 13% and is relatively constant from year to year.

The question arises: do these similar deposition patterns correspond to invariable meteorologic patterns in the years 1978-82? Insight to this question is provided by den Tonkelaar (1985) who has analyzed meteorologic differences between these years by analyzing the frequency of occurrence of *Grosswetterlagen*, (GWL) i.e. synoptic-scale circulation patterns. Since these Grosswetterlagen are related to precipitation and wind patterns, their frequency of occurrence within a year provides a useful indirect

Table 7.4 Summary of computed mean absolute deviations and mean relative deviations.

Scenario	Country	Mean Absolute Deviation (g m^2 yr^{-1})				Mean Relative Deviation (%)			
	Matrix →	7879	7980	8081	8182	7879	7980	8081	8182
Yr 1980	U.K.	.277	.244	.261	.233	10.90	9.61	10.27	9.18
	U.S.S.R.	.329	.374	.322	.394	13.06	14.85	12.81	15.67
	Yugoslavia	.734	.439	.442	.518	15.06	9.00	9.06	10.62
	Europe	.345	.317	.324	.351	12.92	11.89	12.16	13.18
Yr 2010 Major Pollution Controls	U.K.	.119	.100	.110	.109	10.58	8.93	9.77	9.68
	U.S.S.R.	.122	.154	.125	.191	13.61	17.21	14.00	21.34
	Yugoslavia	.255	.154	.155	.191	15.13	9.15	9.16	11.33
	Europe	.132	.128	.127	.155	12.99	12.60	12.48	15.20

basis for comparing the gross climate patterns of different years. Den Tonkelaar (1985) used 13 categories of Grosswetterlagen in his analysis, and noted the number of days in which each Grosswetterlage occurred. He analyzed each of the four annual periods of the EMEP source-receptor matrices (Table 7.5). He then compared the frequency of occurrence of Grosswetterlage for each of these years with their long term (1949-80) annual occurrence. He also compared the four-year (October 1978-September 1982) average annual occurrence with the long term annual occurrence. An example of his results is presented in Table 7.5. *Preliminary* conclusions of den Tonkelaar's analysis are:

1. The four year annual average (October 1978-September 1982) was climatologically similar to the long term (1949-1980) annual average.
2. The climate patterns of the individual years (Table 7.1) departed significantly from one another and from the long term average.

In short, GWL records suggest that the interannual meteorologic variability which occurred within the period of October 1978 to September 1982 was significant from a meteorologic point of view. However, as we have seen, this variability does not create a large difference in forecasted patterns of total sulfur deposition when these patterns are averaged over all of Europe and an entire year.

There are a number of possible reasons for this:

Table 7.5. Occurrence of Grosswetterlage for October 1978-September 1979 and Annual Average 1949-80.

Category of Grosswetterlage[b]	Number of Days	
	October 1978-September 1979	Annual average 1949-1980
1	89	82
2	65	29
3	15	24
4	17	24
5	25	39
6	7	25
7	38	26
8	13	12
9	13	13
10	26	27
11	19	21
12	0	12
13	3	4

[a]Source: den Tonkelaar (1985).

[b]For an explanation of these categories see den Tonkelaar (1985).

(i) *The EMEP model is not sensitive to interannual meteorologic changes.* For example, the EMEP model version upon which this paper is based, assumes a constant mixing height throughout the year and from year to year.* As a result the EMEP model may "smooth out" differences between computed sulfur deposition which would occur from year to year due to changes in average mixing height. On the other hand, the interannual variation of mixing heights is not known, nor is it known whether this would affect interannual sulfur deposition variability.

*Newer versions of the EMEP model are expected to include variable mixing heights.

(ii) *The actual meteorology did not vary much in the years 1978 to 1982.* This would imply that the frequency of *Grosswetterlagen* are not reliable indicators of interannual meteorological variability. One way to check this would be to examine the correlation between wind and precipitation data at several stations and the occurrence of *Grosswetterlagen*.

(iii) *Deposition is compensated by sulfur emission sources and/or wind and precipitation.* Assuming the EMEP model does adequately incorporate the main effects of interannual meteorological variability on sulfur deposition, and assuming this variability was significant between 1978-82, then the relatively low variability of sulfur deposition may be due to compensation between sulfur emission sources, i.e. if prevailing winds transport sulfur from source 'A' to receptor 'B' in one year, then in the next year prevailing winds from a different direction bring the same amount of sulfur to receptor 'B', but from a different source, 'C'. Using Southern Sweden as a receptor example, perhaps the principal source of sulfur in one year will be U.K. and the next year Poland, but the net difference in deposition will be small.

Another type of compensation could result from meteorological factors. For example, if precipitation at receptor 'B' is much lower than usual during a particular year, the reduction in wet deposition may be compensated by longer range transport of sulfur to this receptor location from more distant sulfur sources. It is also possible that (i) through (iii) occur in some combination.

Using the same data base as above we can also compare how the magnitude of interannual variability affects sulfur deposition on different time and space scales. Figure 7.1 summarizes these results for the case of U.K. sulfur emissions and deposition into a single EMEP grid element in Southern Sweden (Rörvik). Results from this analysis (Figure 7.1) show that there is a great difference in mean relative deviation for the combination of monthly country emissions and monthly grid deposition versus annual country emissions and annual grid deposition (mrd = 64.1% vs 8.5%). However this example is useful for only illustrative purposes since it was based on only four data points from the four simulation years.

Conclusions of Matrix Analysis

(i) The *rms* of the computed sulfur deposition matrices depend on the prescribed sulfur emission scenario. Therefore, to identify the matrix with "highest" interannual meteorological variability, we must also estimate the geographic pattern of sulfur emissions.

(ii) The absolute deviation from year-to-year of sulfur deposition in a grid element depends, of course, on the magnitude of sulfur emissions. The absolute deviation in any single grid element spatially varied from about .06 to .25 g m^{-2} yr^{-1} for the lowest sulfur emission scenario and from about 1.0 to 6.0 g m^{-2} yr^{-1} for the highest scenario.

(iii) The relative deviation of sulfur deposition in any single grid element varied spatially by about 5 to 20%.

(iv) The average grid element in Europe had a relative deviation of about 13%. This European-average was fairly consistent from year-to-year for the four years examined.

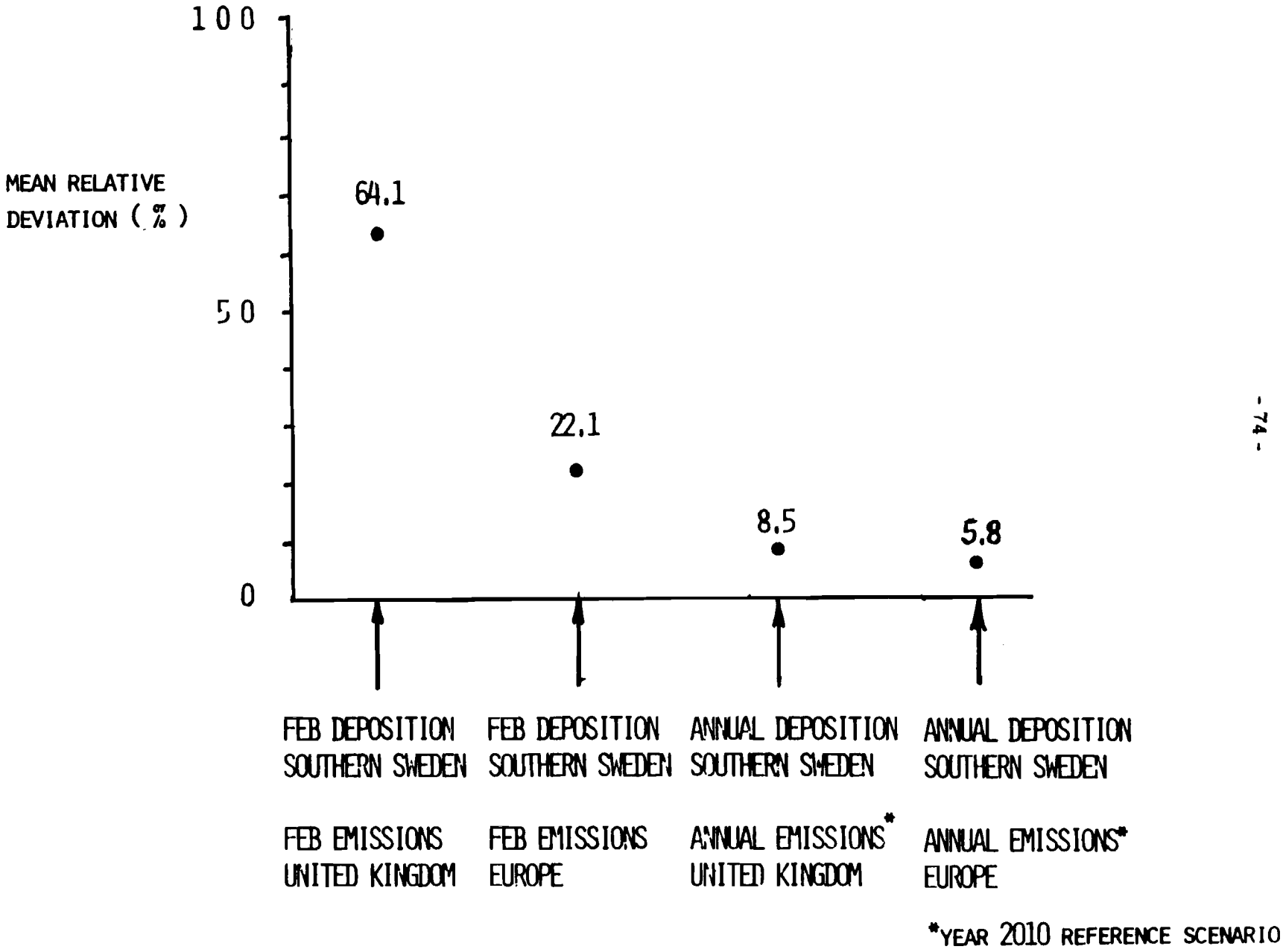

Figure 7.1. **Interannual variability of sulfur deposition affected by different time and space scales.**

Comparison of Uncertainty due to Interannual Meteorological Variability with Uncertainty due to Parameters

In Section 6.5 we present some preliminary results of uncertainty in computed total sulfur deposition due to uncertainty of parameters v_d, h, k_t, and k_w as expressed in frequency distributions in Figure 6.3b. In that example we looked at the combination of U.K. emissions and Southern Sweden (Rörvik) deposition for 1980 environmental and sulfur emission conditions. We can compare this parameter uncertainty with the uncertainty due to interannual meteorological variability by using the data base quoted above and computing the mean deposition from the four unit source-receptor matrices (.216) and a standard deviation (.025) which yields a coefficient of variation of .12. We compare parameter and meteorologic uncertainties for this source-receptor combination and 1980 environmental conditions and find:

coefficient of variation (interannual meteorologic uncertainty)	=	.12
coefficient of variation (parameter uncertainty)	=	.09

In this case they are of the same order of magnitude. However, as noted above, the estimate of interannual meteorologic variability was based on very little data and should therefore only be used for illustration. Similar computations for several other stations would add more statistical validity to the comparison of meteorological variability uncertainty with other types of uncertainty.

7.3. Future Work

Section 7 only outlines the analysis of forecasting uncertainty of the EMEP model. The analysis of model structure uncertainty will include experimentation with different functional forms of the sulfur long range transport equations. The investigation of interannual meteorological variability will include, for example, the analysis of historical climatic data as outlined in Section 7.2.1. This investigation will also be extended to include:

(i) A study of the correlation between *grosswetterlagen* and observations of wind velocities and precipitation.

(ii) Statistical comparison of annual frequency of occurrence of *grosswetterlagen* in the 1978-82 period and their long term annual frequency of occurrence.

(iii) Statistical analysis of results from SO_2 and $SO_4^=$ air concentration matrices from EMEP.

(iv) Comparison of results from "climatic" standard source-receptor matrix with other matrices.

8. APPLICATION TO DECISION MAKING

Once we have assembled quantitative estimates of uncertainty of long range air pollutant transport models, we must still translate this information into a form suitable for decision making. Specifically, we would like to incorporate uncertainty information in computer tools used by policy analysts. There are a variety of ways to accomplish this.

8.1. Parallel Models

An obvious way to include uncertainty information in decision making is to provide policy analysts with a convenient way to use alternative models for analysis of control strategies. If we can accept the assumption of linearity between sulfur emissions and deposition, then information from LRTAP models can be concisely summarized in so-called *source-receptor* or *transfer* matrices. These matrices describe the relationship between sulfur deposition* at a particular location due to the sulfur emissions at another location. Spatial and temporal scales of this matrix depend on its application. For example the matrix used for analysis of control strategies in the IIASA RAINS model (see, e.g. Alcamo et al 1985, and Hordijk, 1985) has country emissions, grid element deposition and an annual time scale.

It is feasible to assemble source-receptor matrices from a number of models and make them available for interactive policy analysis. This approach is being included in the RAINS model. As noted in Section 6.2, comparison of output from different models will yield information about model structure uncertainty but will say little about parameter and other uncertainty.

*Or, in principle, any of the other model state variables such as SO_2 air concentration.

We can, however, examine the possible effect of interannual meteorological variability by comparing results from different source-receptor matrices based on the same model but with different meteorological input. Recall that in Section 7 we used 4 annual source-receptor matrices to investigate uncertainty which may be attributed* to interannual meteorological variability. These four annual matrices have also been implemented for routine use in the RAINS model and are used to calculate deposition. Figure 8.1. compares the sulfur deposition calculated by using the four different matrices for a particular sulfur emission scenario.

A variation of this approach would be to use a "climatologically standard"** source receptor matrix for routine calculations which accounts for interannual meteorological fluctuations. Results from this "standard" matrix could be compared, for example, to results from the four annual matrices mentioned above, in order to estimate the possible effect of interannual meteorological variability. This approach has been developed by den Tonkelaar (1985).

8.2. Uncertainty Ranges

Another simple approach to the problem of incorporating uncertainty information in decision making is to assign uncertainty ranges (ε in this paper) to elements of a source-receptor matrix. This uncertainty range could be a confidence interval, a standard deviation, or other statistical measure of the frequency distributions of sulfur deposition, concentration,

*In Section 7 we noted that it is not certain whether the interannual variability of sulfur deposition as computed in model experiments is positively due to meteorological factors, though it is suspected to be.

**This matrix is "climatologically standard" in that it reflects source-receptor relationships which result from long-term averages of meteorological variables.

etc., presented throughout this paper. The question of which statistic is most appropriate as a standard of model uncertainty is very important but is outside the scope of this paper.

As an example of this approach we present Figures 8.2 and 8.3 which show the effect of a ±13% uncertainty range on computed sulfur deposition.* The effects of this uncertainty range vary greatly spatially (Figure 8.2) and temporally (Figure 8.3). This is probably due to the complex relationship between deposition and the geographic patterns of sulfur emissions, background deposition, and other factors. Figures 8.2 and 8.3 translate uncertainty into a form relevant to policy analysis. For example, Figure 8.2 indicates by how many kilometers a particular deposition computation could vary (based on a ±13% uncertainty range). Figure 8.3 portrays the shift in the percentage of European area where total sulfur deposition is above a specified level; also for ±13% uncertainty range.

By comparing Figures 8.2a and 8.2b and 8.3a and 8.3b, one can also see how much the effect of a ±13% uncertainty depends on the deposition level and location of interest. We can also deduce that the effect of this uncertainty depends on sulfur emission levels, since it is only sulfur emission levels which change with time in Figures 8.3a and b. The change in the width of these lines with time (i.e. their uncertainty) must therefore be due only to changing sulfur emissions.

*The ±13% uncertainty range is based on the European-mean relative deviation of annual sulfur deposition computed in Section 7 and thought to be due to interannual meteorological variability.

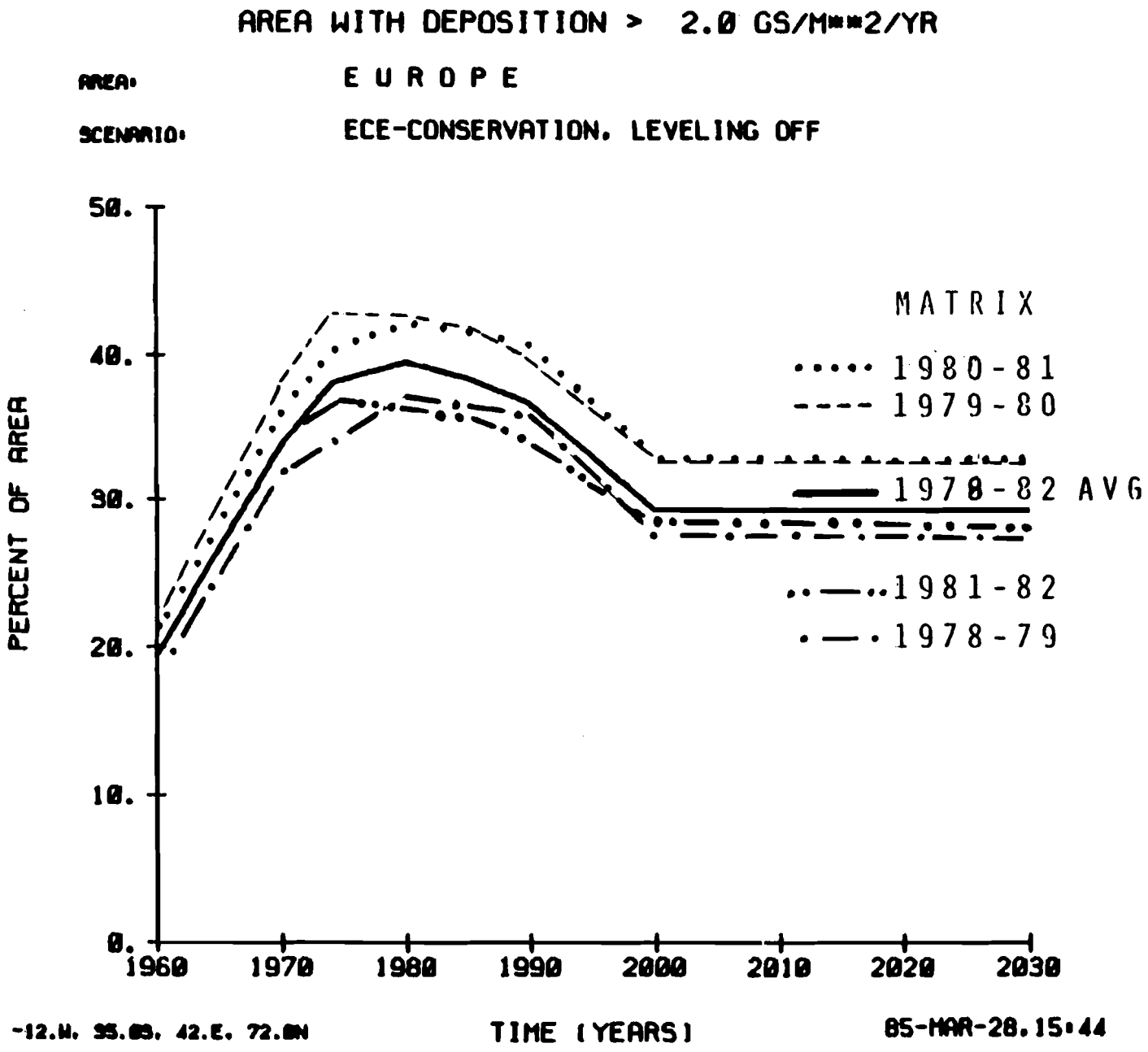

Figure 8.1. Computed area of deposition > 2.0 $g\ m^{-2}\ yr^{-1}$ using five source-receptor matrices based on different meteorologic inputs.

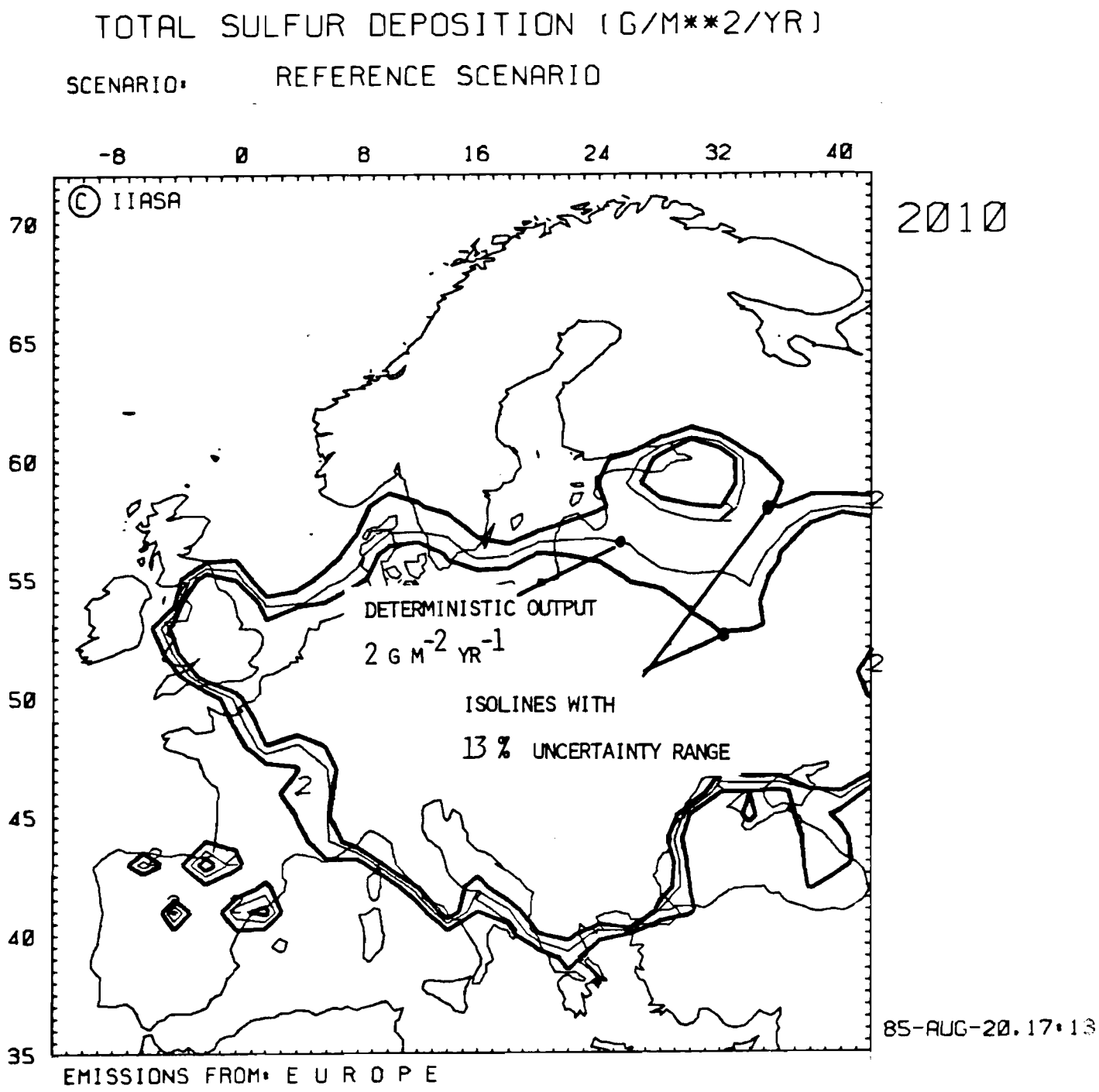

Figure 8.2a. Computed 2 $g\ m^{-2}\ yr^{-1}$ deposition isoline with uncertainty due to ± 13% model uncertainty.

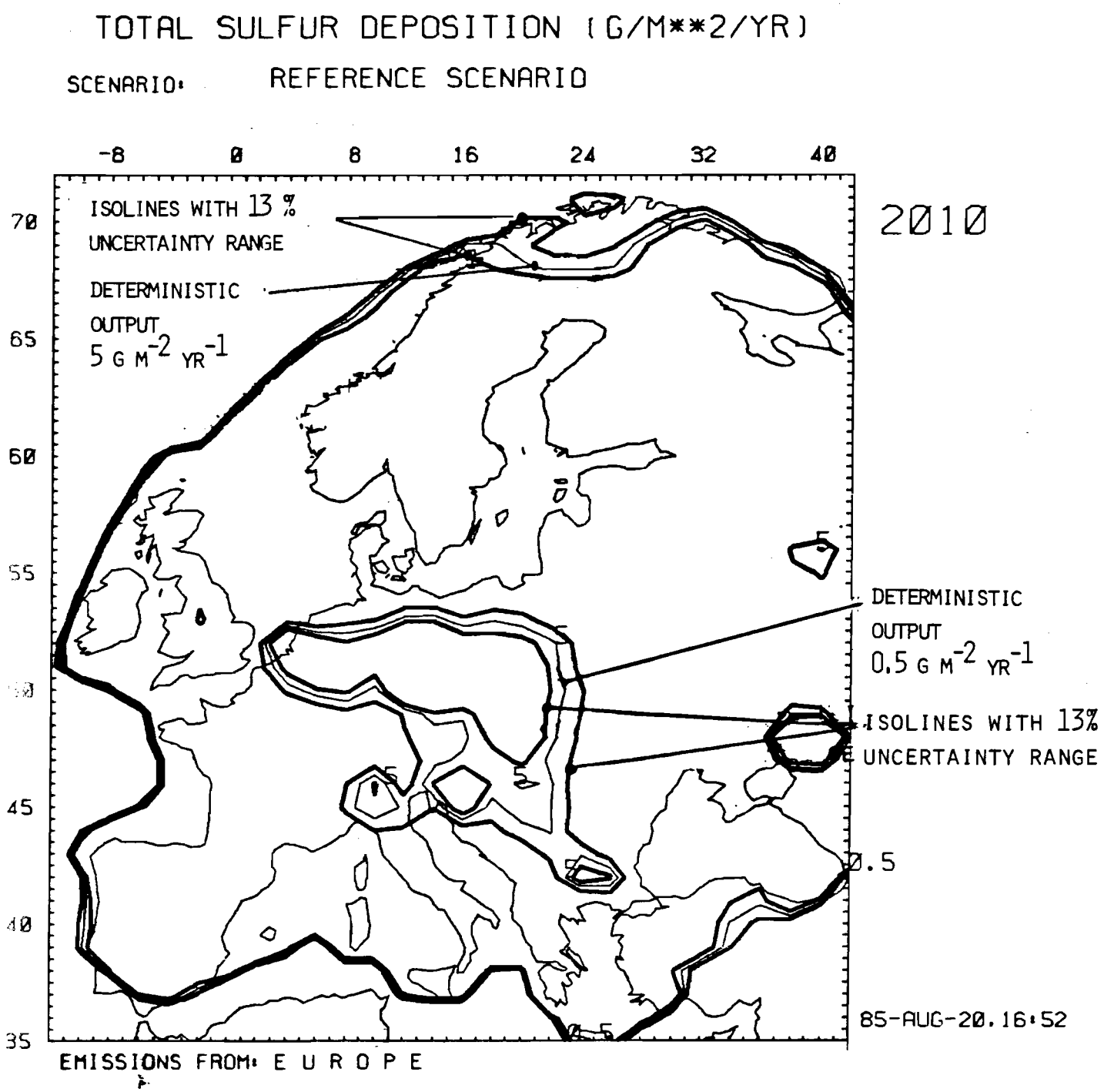

Figure 8.2b. Same as Figure 8.2a except for 0.5 and 5.0 $g\ m^{-2}\ yr^{-1}$ deposition isoline.

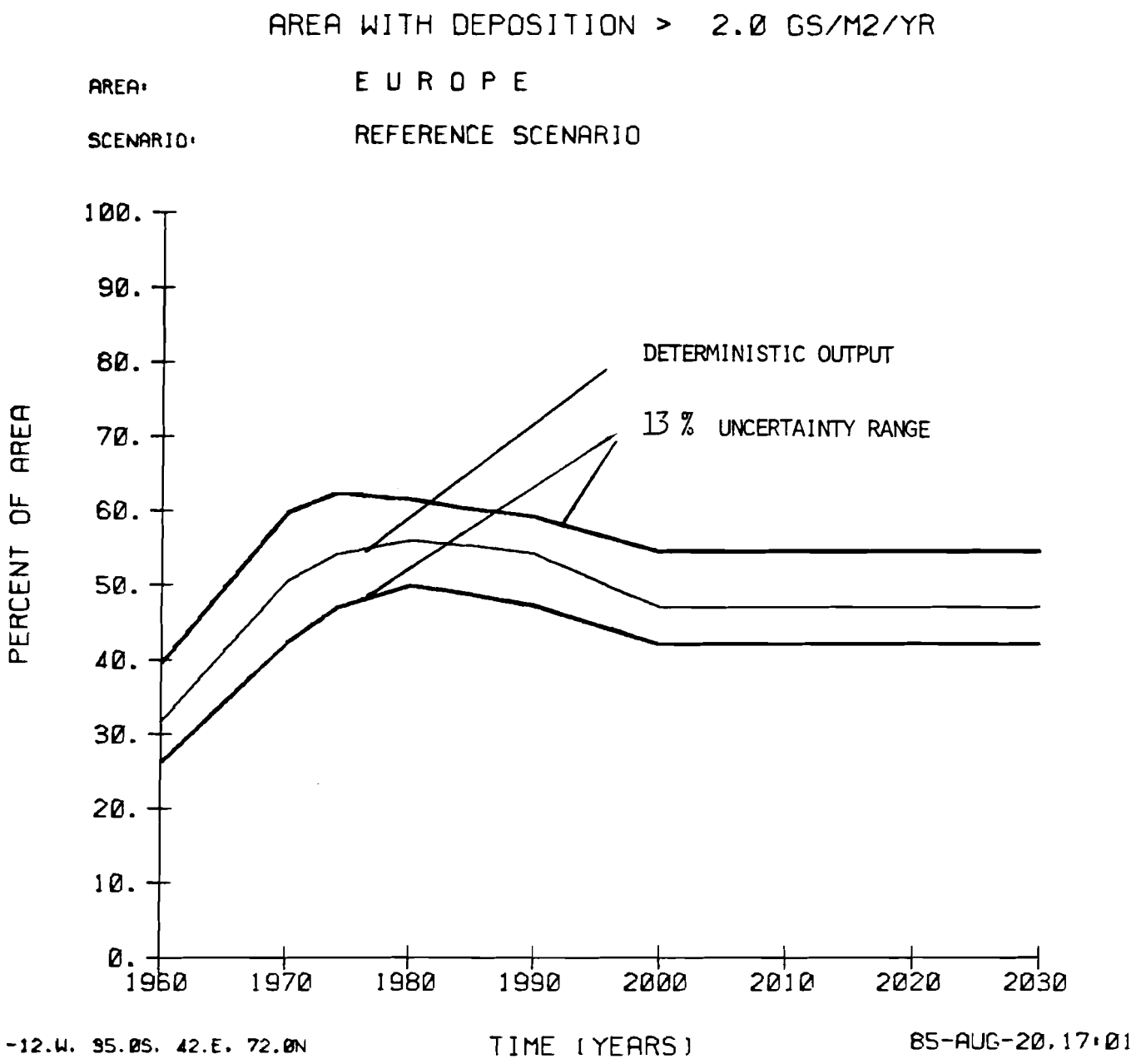

Figure 8.3a. Computed area of deposition > 2.0 $g\ m^{-2}\ yr^{-1}$ with uncertainty due to ± 13% model uncertainty.

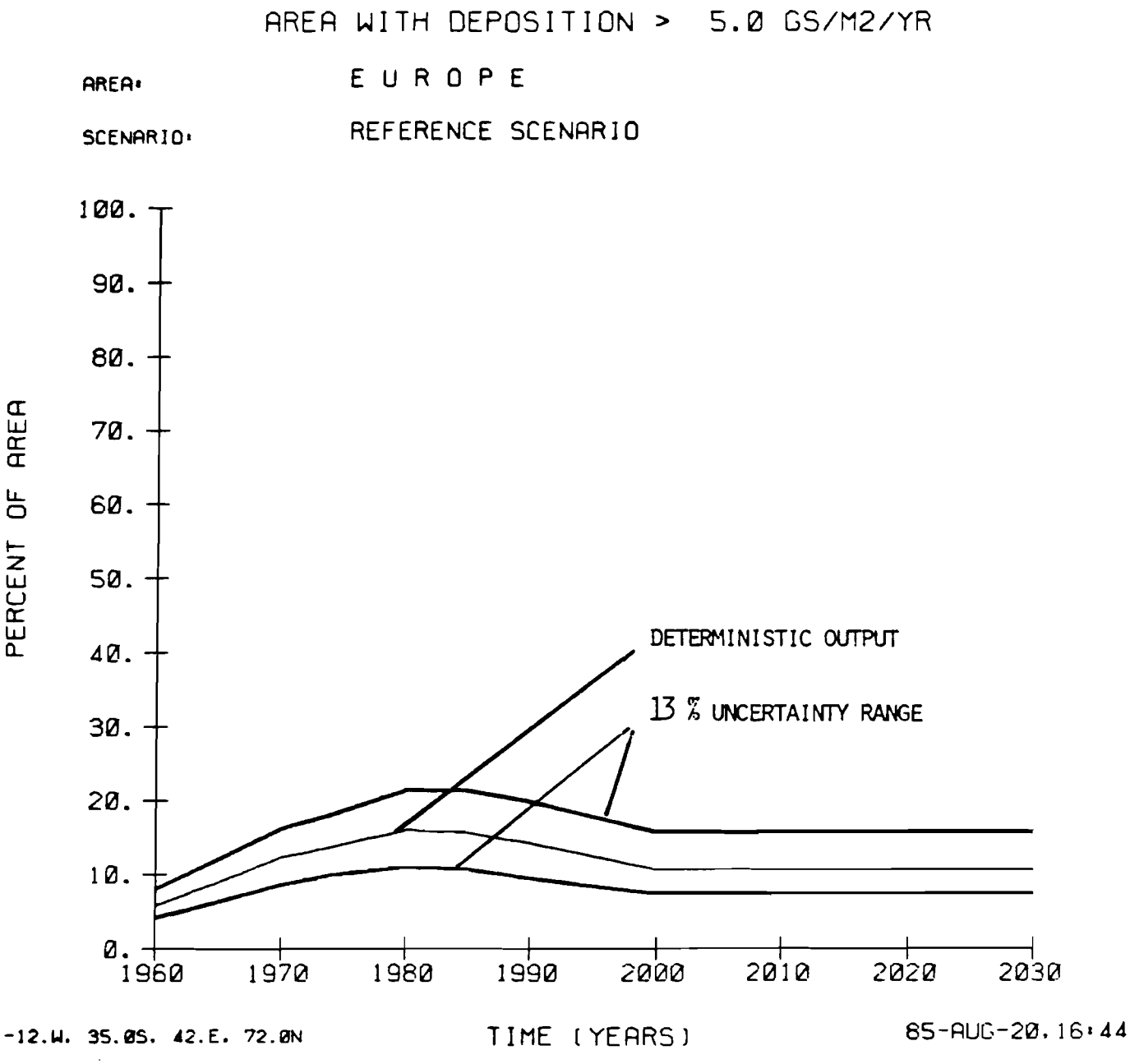

Figure 8.3b. Same as Figure 8.3a except for 5.0 $g\ m^{-2}\ yr^{-1}$.

9. CONCLUSIONS

In this paper we have assembled ideas relevant to assessing the uncertainty of a long range air pollutant transport model. We have also taken the first steps in organizing these ideas into a comprehensive framework for model uncertainty analysis and have applied this framework to EMEP model uncertainty. Since this research is in its early stages, we have described plans for future work in Sections 6.4 and 7.3.

The following are conclusions we have reached to this point:

(i) There is a distinction between uncertainty analysis, sensitivity analysis and calibration/verification. However, sensitivity analysis and calibration/verification have a role in uncertainty analysis, apart from their importance in model development (Section 1.2).

(ii) Sensitivity analysis can be used for "screening and ranking" uncertainty sources, i.e. to limit the number of uncertainty sources which must be quantitatively evaluated (Section 1.2).

(iii) Information from model calibration/verification (i.e. comparing model output with observations) cannot be directly used to quantify model uncertainty. However, observations can be used to indirectly check the uncertainty analysis procedure (Sections 2.1, 6.1).

(iv) The taxonomy of model uncertainty presented in this paper was useful for organizing uncertainties of the EMEP model (Section 4.2).

(v) A method was presented to analyze "composite" uncertainty (parameters, forcing functions and initial state) which uses Monte Carlo simulation. In preliminary applications, we found this method to be a general and flexible way of examining this composite uncertainty (Section 6.3).

(vi) Using the above Monte Carlo method, we investigated the composite effect of uncertainty of the dry deposition rate (v_d), mixing height (h), SO_2 transformation rate (k_t) and SO_2 wet deposition rate (k_w). This model experiment was conducted for the United Kingdom as a sulfur source and Southern Sweden as a sulfur receptor. Meteorologic data from 1980 were used as input and results with an annual time scale were analyzed. The "largest" uncertainty (as defined by the largest coefficient of variation) was observed for computed SO_2 air concentration, the smallest for computed dry deposition. The smaller uncertainty of computed dry deposition can be explained by the way in which the EMEP model computes dry deposition. This may or may not be a good reflection of nature. Of the four parameters tested, k_t created the largest uncertainty (i.e. coefficient of variation) in total annual sulfur deposition. This result depends on the frequency distributions assigned to the parameters. Since model uncertainty estimates are very dependent on these assigned frequency distributions, a large effort will be devoted to improving their estimation (Section 6.3).

(vii) The possible effect of interannual meteorological variability on uncertainty of EMEP calculations was investigated by statistical analysis of results from EMEP source-receptor matrices. We found that the effect of interannual meteorological variability strongly depends on the geographic pattern and magnitude of sulfur emissions. We also found that the mean relative deviation of sulfur deposition in all European grid elements, in a four-year period between 1978–82, was approximately 13%. As discussed in the text, these results are possibly, but not positively, related to interannual meteorological variability (Section 7.2).

(viii) An uncertainty which is expressed in *constant* percentage terms, e.g. "the uncertainty range of each grid element is ± 13% of the mean computed deposition", can have a widely-varying spatial and temporal effect on computed sulfur deposition patterns in Europe. The effect depends on the location, deposition level, and sulfur emission pattern (Section 8).

REFERENCES

Alcamo, J., L. Hordijk, J. Kämäri, P. Kauppi, M. Posch and E. Runca. 1985. Integrated analysis of acidification in Europe. *Journal of Env. Manag. 21*, 47-61.

Anon. 1983. EMEP/MSC-W Report 1/83.

Bartnicki, J. and J. Alcamo (forthcoming). A review of sensitivity tests of the EMEP model. IIASA Working paper, A-2361 Laxenburg, Austria.

Bartnicki, J., J. Kucharszuk and J. Alcamo (forthcoming). Uncertainty due to model operation in the EMEP approach to long range transport of air pollutants. IIASA Working Paper, A-2361 Laxenburg, Austria.

Beck, M.B., and G. van Straten (eds.) 1983. *Uncertainty and forecasting of water quality*. Springer-Verlag: Berlin.

Bhumralkar, M.B., R.M. Endlich, R. Brodzinsky, K.C. Nitz and W.B. Johnson. 1982. Further studies to develop and apply long- and short-term models to calculate regional patterns and transfrontier exchange of airborne pollution in Europe. Final Report, SRI Project 8365, SRI International.

den Tonkelaar, J. 1985. Deposition of sulfur in Europe. TR-66 Technical Report of the Dutch Meteorological Institute (KNMI), Fysische Meteorologie, Postbus 201, 3730 AE, de Bilt, Netherlands.

Dovland, H., and J. Saltbones. 1979. Emissions of sulphur dioxide in Europe in 1978. EMEP/CCC Report 2/79.

Eliassen, A. 1978. The OECD study of long range transport of air pollutants: long range transport modelling. *Atmos. Environ. 12:* 479-487.

Eliassen, A., and J. Saltbones. 1975. Decay and transformation rates of SO_2 as estimated from emission data trajectories and measured air concentrations. *Atmos. Environ., 9:* 425-429.

Eliassen, A., and J. Saltbones. 1983. Modeling of long range transport of sulfur over Europe: a two-year model run and some model experiments. *Atmos. Environ. 17:* 1457-1473.

Fedra, K. 1983. Environmental modeling under uncertainty: monte carlo simulation. IIASA Research Report, RR-83-28, A-2361, Laxenburg, Austria.

Fox, D.G. 1984. Uncertainty in air quality modeling. *Bull. Am. Meteor. Society 65* (1): 27-36.

Gardner, R.H., W.G. Cale and R.V. O'Neill. 1982. Robust analysis of aggregation error. *Ecology 63* (6): 1771-1779.

Granat, L. 1978. Sulfate in precipitation as observed by the European atmospheric chemistry network. *Atmos. Environ. 12:* 413-424.

Griliches, Z., and M.D. Intrilligator (eds.). 1983. *Handbook of econometrics, Vol. I.* North Holland: Amsterdam.

Hordijk, L. 1985. A model for evaluation of acid deposition in Europe. in: *Systems analysis and simulation 1985, volume II: applications.* Akademie-Verlag: Berlin. pp. 30-39.

Howard, R.E., and J.E. Matheson (eds.). 1983. *Principles and application of decision analysis, Vol I: general collection.* Strategic Decision Group: Menlo Park, California.

Lamb, R.G. 1984. Air pollution models as descriptors of cause-effect relationships. *Atmos. Environ. 18* (3): 591-606.

McLeod, J. 1982. Computer modeling and simulation - principles of good practice. Simulation Councils, Inc.: LaJolla, California.

MOI, 1982. (Memorandum of Intent on Transboundary Air Pollution). Work group 2, atmospheric sciences and analysis. Report No. 2F-M.

Morgan, M.G., S.C. Morris, M. Henrion, D.A.L. Amaral and W.R. Rish. 1984. Technical uncertainty in quantitative policy analysis - a sulfur pollution example. *Risk Analysis 4* (3): 201-216.

OECD (Organization for Economic Cooperation and Development). 1979. Long range transport of air pollutants. OECD: Paris.

Oppenheimer, M., C. Epstein, R. Yuhnke. 1985. Acid deposition, smelter emissions and the linearity issue in the Western U.S. *Science. 229:* 859-862.

OTA (Office of Technology Assessment). 1984. Acid rain and transported air pollutants: implications for public policy. OTA-0-204. U.S. Superintendent of Documents, U.S. Govt. Printing Office, Washington, D.C. 20402.

Petterssen, S. 1956. *Weather analysis and forecasting*. McGraw-Hill: New York.

Pitovranov, S. *(forthcoming)*. A method to assess the effect of possible climate change on sulfur deposition patterns in Europe. In: Alcamo, J., and J. Bartnicki (eds.), Summary report of technical meeting on atmospheric computation for assessment of acidification in Europe: work in progress. Warsaw, 4-5 September 1985.

Prahm, L.P., O. Christensen. 1977. Long-range transmission of pollutants simulated by the 2-D pseudospectral disperson model. *Journ. of Appl. Meteor. 16:* 896-910.

Streets, D.G., B.M. Lesht, J.D. Shannon and T.D. Veselka, 1985. Climatological variability. *Environ. Sci. Tech. 19* (10): 887-893.

U.S. National Research Council. 1983. Acid deposition, atmospheric processes in North America. National Academy Press: Washington, D.C.

WMO, 1983. Expert meeting on the meteorological aspects of the second phase of EMEP (mimeo). Geneva: United Nations World Meteorological Organisation.